

A comprehensive analysis of gene expression profiles in distal parts of the mouse renal tubule

Sylvain Pradervand · Annie Zuber Mercier ·
Gabriel Centeno · Olivier Bonny · Dmitri Firsov

Received: 12 May 2010 / Revised: 5 July 2010 / Accepted: 5 July 2010 / Published online: 5 August 2010
© Springer-Verlag 2010

Abstract The distal parts of the renal tubule play a critical role in maintaining homeostasis of extracellular fluids. In this review, we present an in-depth analysis of microarray-based gene expression profiles available for microdissected mouse distal nephron segments, i.e., the distal convoluted tubule (DCT) and the connecting tubule (CNT), and for the cortical portion of the collecting duct (CCD; Zuber et al., Proc Natl Acad Sci USA 106:16523–16528, 2009). Classification of expressed transcripts in 14 major functional gene categories demonstrated that all principal proteins involved in maintaining the salt and water balance are represented by highly abundant transcripts. However, a significant number of transcripts belonging, for instance, to categories of G-protein-coupled receptors or serine/threonine kinases exhibit high expression levels but remain unassigned to a specific renal function. We also established a list of genes differen-

tially expressed between the DCT/CNT and the CCD. This list is enriched by genes related to segment-specific transport functions and by transcription factors directing the development of the distal nephron or collecting ducts. Collectively, this *in silico* analysis provides comprehensive information about relative abundance and tissue specificity of the DCT/CNT and the CCD expressed transcripts and identifies new candidate genes for renal homeostasis.

Keywords Kidney · Homeostasis · Membrane transport · Transport · Urinary excretion

Introduction

The final adjustment of urine composition takes place in the distal parts of the renal tubule, i.e., in the distal nephron and in the collecting duct. Over the last decades, research efforts in the field allowed identification of many essential proteins (channels, transporters, receptors, etc.) involved in this process. The majority of these proteins were first discovered by expression cloning, an approach based on the a priori available information about function and tissue expression distribution of the candidate gene. The aquaporin-2 water channel (aqp-2), the V₂-type of vasopressin receptor (Avpr2), the Ca²⁺-sensing receptor (CaSR), the thiazide-sensitive sodium chloride cotransporter (NCC), the secretory potassium channel (ROMK), the amiloride-sensitive sodium channel (ENaC), and the epithelial calcium channel (Trpv5) are just a few out of many examples of proteins identified by this approach. Moreover, a growing list of functionally important genes has been added from human genetic association studies. The latter includes WNK1 and WNK4 serine/threonine kinases [1], the FXRD2 subunit of the Na₃K-ATPase [2], the KCNJ10 and KCNA1 potassium channels, and the pro-EGF [3–5]. Significant progress in deciphering

Olivier Bonny and Dmitri Firsov have equally contributed to the study.

Electronic supplementary material The online version of this article (doi:10.1007/s00424-010-0863-8) contains supplementary material, which is available to authorized users.

A. Zuber Mercier · G. Centeno · O. Bonny (✉) · D. Firsov (✉)
Department of Pharmacology and Toxicology,
University of Lausanne,
27 rue du Bugnon,
1005 Lausanne, Switzerland
e-mail: olivier.bonny@unil.ch
e-mail: dmitri.firsov@unil.ch

S. Pradervand
Lausanne Genomic Technologies Facility,
Center for Integrative Genomics,
University of Lausanne,
1015 Lausanne, Switzerland

O. Bonny
Service of Nephrology, Lausanne University Hospital,
1011 Lausanne, Switzerland

regulatory pathways in the distal nephron and/or collecting ducts has been made with the development of methods allowing global view of all expressed transcripts (transcriptome) or proteins (proteome) and their dynamics. For example, the aldosterone or vasopressin signaling pathways were extensively characterized by the serial analysis of gene expression and microarray hybridization [6, 7]. Various proteome tools were used for identification of vasopressin-dependent phosphorylation sites within aqp-2 or for detection of lithium-induced changes in the proteome of the inner medullary collecting ducts (IMCD) [8, 9].

In order to identify new genes involved in renal homeostatic mechanisms, we used an *in silico* approach based on the analysis of transcript abundance in several major functional gene categories most relevant to secretion/reabsorption processes in the distal nephron and/or the collecting duct. This analysis was performed on a recently obtained microarray-based dataset of gene expression profiles of the mouse distal convoluted tubule (DCT), the connecting tubule (CNT), and the cortical collecting duct (CCD) [10]. The principal characteristics of this dataset are the following: (1) the DCT/CNT and the CCD samples were obtained by microdissection; the DCT and CNT were microdissected together because of the gradual transition between these two segments in mice; (2) samples were prepared from animals sacrificed for microdissection every 4 h throughout a 12 h/12 h light–dark cycle (a total of six time points); this protocol allows detection of all expressed transcripts independently of diurnal variations in their expression levels; (3) a total of 30 animals were used for microdissection of DCT/CNT and CCD samples (five animals per time point); (4) 12 microarray hybridizations were performed for both DCT/CNT and CCD (two hybridizations per time point). The quality of microdissection was validated by the analysis of expression levels of several nephron segment-enriched transcripts (see [10] and below). Altogether, this dataset represents a complete and reliable source of information on the genes expressed in the distal nephron and the CCD (see below).

Functional classification and analysis of transcript abundance allowed us to identify a new set of highly abundant transcripts encoding proteins potentially relevant to the homeostasis of water and/or electrolytes. Finally, comparison of the DCT/CNT and the CCD transcriptomes revealed a number of previously uncharacterized transcripts exhibiting significantly different expression levels between these parts of the renal tubule. These data could be further used for the functional characterization of the identified candidates.

Functional classification of DCT/CNT and CCD transcripts

Functional classification of DCT/CNT and CCD transcripts was performed using the PANTHER Classification System, a database allowing subdivision of proteins and mRNA tran-

scripts into functionally related categories (www.pantherdb.org). A similar approach was previously used by Uawithya et al. for the transcriptional profiling of rat IMCD [11]. The classification data are presented in tables in which only the 20 most abundant transcripts per category are listed for space purposes. If more than 20 transcripts per category fitted the cutoff criteria (see below), a full list of transcripts can be viewed in associated supplementary tables. The transcripts are ranked by their abundance calculated as log₂ normalized microarray hybridization signal intensity (*A* values) [12]. Hence, a difference in one unit of *A* values corresponds to the twofold difference in the transcript expression levels. The median microarray signal intensity (5.8 units of *A* value, for both the DCT/CNT and the CCD transcriptomes) was chosen as an arbitrary cutoff value above which expression of a transcript was assigned as significant. The data are discussed in terms of expression levels or transcripts abundance. However, we have to emphasize that microarray signal intensities and sequencing-based quantification of mRNA abundance have been shown to exhibit a correlation coefficient of ~0.7 [13]. To assess this correlation in the DCT/CNT and the CCD datasets, we performed qPCR analysis of transcripts abundance in one of the selected gene categories, namely G-protein-coupled receptors (GPCR). As shown in Fig. 1a, b, both DCT/CNT and CCD datasets exhibit a good correlation between microarray signal intensities and Ct values of qPCR amplification (correlation coefficients of 0.769 and 0.823, respectively). These data also demonstrate that transcripts with *A* values below the median cutoff level exhibit significantly lower correlation between microarray and qPCR data.

G-protein-coupled receptors

Most GPCRs that have been previously identified in the DCT/CNT and/or the CCD are abundantly represented in the respective transcriptomes (Table 1 and Supplemental Table 1). These include vasopressin receptors type 1a (Avpr1a) and type 2 (Avpr2), prostaglandin E receptors type 3 (Ptger3), type 1 (Ptger1), and type 4, prostaglandin F receptor (Ptgfr), glucagon receptor (Gcgr), proteinase-activated receptor 2 (F2rl1), CaSR, endothelin receptor type B (Ednrb), parathyroid hormone receptor 1 (Pth1r), adenosine A1 receptor, and adrenergic receptors type beta 1, beta 2, and alpha 2a. This analysis also revealed the presence of a number of highly abundant GPCRs with yet unassigned function in the kidney. For instance, both DCT/CNT and CCD exhibit high expression levels of several chemokine GPCRs, including Ccr11, Cxcr4, and Gpr146. The Cxcr4 receptor has been shown to bind SDF-1, a chemokine involved in a multitude of functions, including epithelial patterning and renal morphogenesis [14]. However, the role of chemokine GPCRs in the adult kidney remains unknown. The DCT/CNT and the CCD transcriptomes are enriched by orphan

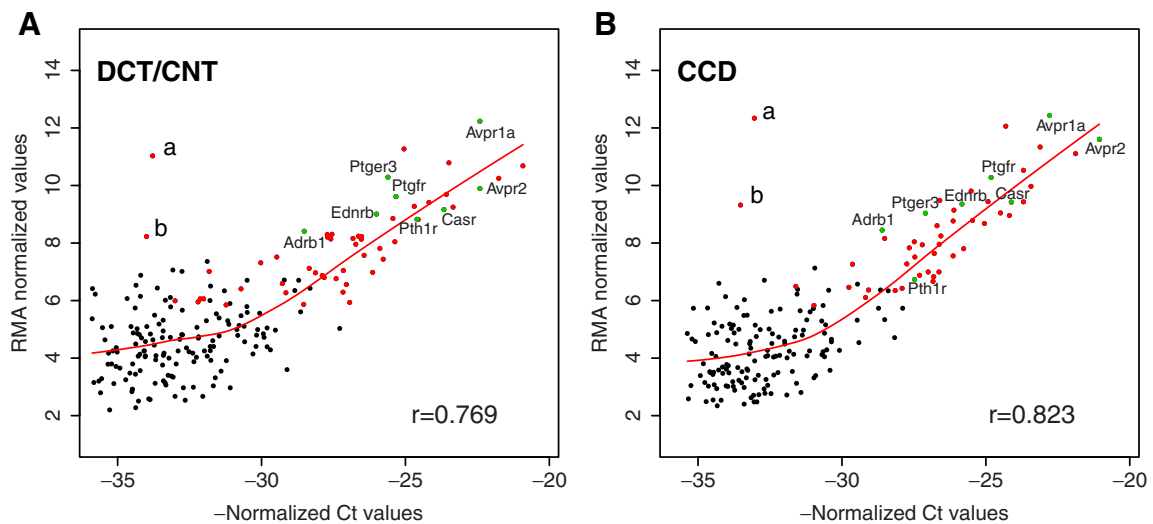


Fig. 1 Correlation between qPCR- and microarray-based expression levels of GPCRs expressed in the DCT/CNT (**a**) and the CCD (**b**). Negative mean normalized Ct values (*x*-axis) are plotted against normalized expression values measured by Affymetrix microarrays (*y*-axis). Genes with the Ct values of 36 or above are not plotted. Loess

curves are indicated with a *red line*. Genes considered as expressed from the microarray data are indicated with a *red dot*. Several genes discussed in the text are indicated with a *green dot*. Two outliers are Cxcr7 (**a**) and Slpr3 (**b**). The qPCR was performed on mouse GPCR array from Applied Biosystems

receptors belonging to a subclass of adhesion GPCRs (Celsr2, Gpr116, Gpr56, and Celsr1). Adhesion GPCRs constitute a novel subclass of GPCRs characterized by the presence in their N termini of cadherin-like cell adhesion modules. These receptors are critical for the normal development of the central nervous system and for the

immune response. Several adhesion GPCRs are involved in human diseases. For example, deletion of the Gpr56 gene in human causes the autosomal recessive bilateral frontoparietal polymicrogyria, a disease characterized by severe neurological dysfunction [15]. However, a renal phenotype in these patients, if any, has not yet been communicated. Both the

Table 1 G-protein-coupled receptors

Gene name	Gene Symbol	DCT/CNT <i>A</i> value	CCD <i>A</i> value
Arginine vasopressin receptor 1A	Avpr1a	12.23	12.44
Cadherin, EGF LAG seven-pass G-type receptor 2	Celsr2	11.27	12.06
Chemokine (C-X-C motif) receptor 7	Cxcr7	11.03	12.34
G-protein-coupled receptor 116	Gpr116	10.79	11.34
G-protein-coupled receptor 56	Gpr56	10.68	11.60
Chemokine (C-X-C motif) receptor 4	Cxcr4	10.39	10.65
Prostaglandin E receptor 3 (subtype EP3)	Ptger3	10.29	9.04
G-protein-coupled receptor, family C, group 5, member C	Gpre5c	10.25	11.11
Arginine vasopressin receptor 2	Avpr2	9.89	11.61
Oxoglutarate (alpha-ketoglutarate) receptor 1	Oxgr1	9.69	9.44
Xenotropic and polytropic retrovirus receptor 1	Xpr1	9.68	9.92
Prostaglandin F receptor	Ptgfr	9.61	10.28
G-protein-coupled receptor, family C, group 5, member B	Gpre5b	9.41	10.53
Glucagon receptor	Gcgr	9.28	8.77
Coagulation factor II (thrombin) receptor-like 1	F2rl1	9.25	9.97
Calcium-sensing receptor	CaSR	9.16	9.42
Endothelin receptor type B	Ednrb	9.01	9.35
Prostaglandin E receptor 1 (subtype EP1)	Ptger1	8.85	9.43
Parathyroid hormone 1 receptor	Pth1r	8.82	6.73
G-protein-coupled receptor 108	Gpr108	8.81	9.05

DCT/CNT and the CCD transcriptomes revealed high expression levels of Gprc5C and Gprc5B, two receptors related to the family C of GPCRs, which also includes the metabotropic glutamate receptors, the GABA(B) receptors, several pheromone receptors, and the calcium-sensing receptor [16]. However, in contrast to other members of the family, both Gprc5C and Gprc5B still remain orphans. Our analysis also revealed a high expression of three receptors belonging to the class A of the rhodopsin-like GPCRs, namely the oxoglutarate receptor 1 (Oxgr1), the estrogen receptor (Gper or Gpr30), and the apelin receptor. Several pieces of evidence indicate that these receptors may have an important role in the regulation of tubular solute transport. Oxgr1 (also known as Gpr80 or Gpr99) is a specific receptor to α -ketoglutarate, a citric acid cycle intermediate [17]. Interestingly, urinary concentration of α -ketoglutarate varies significantly upon perturbation of systemic acid–base balance, being significantly increased in alkalosis and significantly decreased in acidosis [18]. This suggests a possible role for Oxgr1 in sensing acid–base disequilibrium. Gper is a recently identified plasma membrane estrogen receptor which mediates nongenomic effect of estrogen. As it was recently hypothesized, Gper may be involved in the rapid magnesiotropic effects of estrogen in the distal nephron [19]. Apelin is a recently discovered peptide which mediates a multitude of biological functions including vasoconstriction, cardiac myogenesis, glucose metabolism, and vasopressin synthesis/release in the brain. Knockout of apelin receptor in mice leads to abnormal fluid homeostasis, resulting in disturbance of both kidney urinary concentration capacity and drinking behavior [20]. The role of this receptor in the renal tubules has not yet been elucidated.

Heterotrimeric G proteins

GPCRs transduce signals from extracellular stimuli by activating heterotrimeric G proteins. These latter can be grouped into four subfamilies $G\alpha_s$, $G\alpha_i$, $G\alpha_q/11$, and $G\alpha_{12/13}$, according to the structural and functional properties of their α subunits. $G\alpha_s$ and $G\alpha_i$ regulate intracellular cAMP levels by activating ($G\alpha_s$) or inhibiting ($G\alpha_{i1}$, $G\alpha_{i2}$, and $G\alpha_{i3}$) adenylyl cyclase; $G\alpha_q$ and $G\alpha_{11}$ increase intracellular Ca^{2+} level via activation of phospholipase C (PLC); and $G\alpha_{12}$ and $G\alpha_{13}$ couple GPCRs to the small GTPases of the Rho family. As shown in Table 2, all α subunits, with the exception of $G\alpha_{12}$, are well represented in both transcriptomes, thereby providing molecular basis for a variety of intracellular signaling pathways activated by GPCRs in these parts of the renal tubule.

Nucleotide cyclases

Chabardès et al. have shown that cortical and outer medullary collecting ducts exhibit high expression levels

of Ca^{2+} -inhibitable adenylyl cyclases 6 (Adcy6) and 5 (Adcy5) [21]. Our data support these findings and extend the Adcy6 and Adcy5 distribution to the DCT/CNT (Table 3). Both the DCT/CNT and the CCD also show a high expression of Adcy9, a cyclase which can be either potentiated or inhibited by the intracellular Ca^{2+} [22]. Collectively, these cyclases represent a point of crosstalk between the cAMP- and Ca^{2+} -dependent signaling pathways. Similar to what was found in the IMCD, both the DCT/CNT and the CCD exhibit low expression of guanylate cyclases (only Gucyl1a3 fit the cutoff criteria), and none of the nitric acid synthase isoforms were detected (data not shown) [11].

Cyclic nucleotide phosphodiesterases

Cyclic nucleotide phosphodiesterases (Pde) participate in attenuation of GPCR signaling by degrading cellular cAMP and/or cGMP. As shown in Table 4, both the DCT/CNT and the CCD exhibit high expression levels of several cAMP-specific phosphodiesterases, including Ca^{2+} -activated Pde1a and cGMP-inhibited Pde3b. A significant expression of 3-isobutyl-1-methylxanthine (IBMX)-insensitive Pde8a and Pde8b provides a molecular basis for the IBMX-insensitive fraction of phosphodiesterase activity. The rolipram-sensitive cAMP-specific Pde4b and Pde4a have been proposed as important regulators of Avpr2-induced signaling cascade [23]. However, in the DCT/CNT and the CCD transcriptomes presented here, they are expressed only at moderate levels.

Protein kinases

More than 350 protein kinases have been found in the transcriptomes of the DCT/CNT and the CCD (Table 5 and Supplemental Table 2). Most of them (~300, Table 5 and Supplemental Table 2) belong to the class of serine/threonine protein kinases. Importantly, kinases that have been previously reported to strongly influence the secretion/reabsorption processes in DCT/CNT and/or the CCD are abundantly represented. WNK1, WNK4, SPAK (STK39), and Sgk1 have been involved in maintaining salt balance and are present within the 20 most abundant serine/threonine kinases. Both the DCT/CNT and the CCD also exhibit moderate to high expression levels of protein kinase A (Prkaa2, Prkacb, Prkaca, and Prkaa1), protein kinase C (Prkcd, Prkci, Prkch, Prkca, and Prkcz), casein kinases (Csnk1d, Csnk1a1, Csnk2a1, Csnk1g2, and Csnk2a2), Gsk3 β , and G-protein-coupled receptor kinases 6, 5, and 4. Interestingly, several in vitro studies have demonstrated that the activity of the NCC is regulated by WNK3 [24], a kinase which is expressed at background levels in our data (*A* values of 3.8 and 2.8 in DCT/CNT and CCD,

Table 2 Heterotrimeric G proteins

Gene Name	Gene Symbol	DCT/CNT <i>A</i> value	CCD <i>A</i> value
Guanine nucleotide binding protein, alpha stimulating	Gnas	12.34	12.59
Guanine nucleotide binding protein (G protein), beta 1	Gnb1	11.81	12.36
Guanine nucleotide binding protein (G protein), gamma 12	Gng12	11.63	11.64
Guanine nucleotide binding protein, alpha 13	Gna13	10.90	11.22
Guanine nucleotide binding protein (G protein), alpha inhibiting 1	Gnai1	10.84	11.12
Guanine nucleotide binding protein, alpha 11	Gna11	10.65	11.43
Guanine nucleotide binding protein (G protein), gamma 5	Gng5	10.59	11.36
Guanine nucleotide binding protein (G protein), gamma 4	Gng4	10.26	10.72
Guanine nucleotide binding protein (G protein), alpha inhibiting 2	Gnai2	9.92	11.01
Guanine nucleotide binding protein, alpha q polypeptide	Gnaq	9.72	10.27
Guanine nucleotide binding protein (G protein), alpha inhibiting 3	Gnai3	9.62	10.41
Guanine nucleotide binding protein (G protein), beta 4	Gnb4	8.92	9.46
Guanine nucleotide binding protein (G protein), gamma 11	Gng11	8.82	9.23
Guanine nucleotide binding protein (G protein), gamma 10	Gng10	7.62	8.65
Guanine nucleotide binding protein (G protein), beta 5	Gnb5	7.58	7.95
Guanine nucleotide binding protein (G protein), beta 2	Gnb2	7.45	8.48
Guanine nucleotide binding protein (G protein), gamma 2	Gng2	7.31	6.75
Guanine nucleotide binding protein (G protein), gamma 2	Gng2	6.42	5.94
Guanine nucleotide binding protein, alpha z subunit	Gnaz	6.33	6.59
Guanine nucleotide binding protein, alpha 12	Gna12	6.05	6.87

respectively). Accordingly, WNK3 is also absent in microarray-based rat IMCD transcriptome [11]. Collectively, these results indicate that WNK3 distribution in the kidney requires a detailed re-evaluation. By contrast, both the DCT/CNT and the CCD exhibit strong expression of various serine/threonine kinases with yet unattributed function in the kidney. These include Ptk1, Pim3, Pak4, Aak1, Taok3, Rock1, and several MAP kinases. In the kidney, tyrosine kinases (Table 5) and receptor tyrosine kinases (Table 5) have been mostly involved in tubulogenesis, in cell differentiation, and in maintaining cell polarity. However, the fibroblast growth factor receptor 1 (Fgfr1), which is specifically expressed in the distal nephron and the collecting duct, has been recently shown as the predominant receptor for the hypophosphatemic action of fibroblast growth factor 23 [25].

Protein phosphatases

Protein phosphatases participate in intracellular signaling by reversing protein-kinase-dependent events. All protein phosphatases can be grouped into three subfamilies: serine/threonine phosphatases, phosphotyrosine-specific protein tyrosine phosphatases, and dual specificity (serine/threonine/tyrosine) phosphatases. As shown in Table 6 and Supplemental Table 3, both DCT/CNT and CCD express a variety of highly abundant phosphatases representing all three subfamilies. However, despite high expression levels and, presumably, significant functional role, only a limited number of phosphatases have been characterized in the kidney. Several studies have shown that calcineurin (Ppp3ca), a serine/threonine phosphatase with broad substrate specificity, is involved in the

Table 3 Nucleotide cyclases

Gene name	Gene Symbol	DCT/CNT <i>A</i> value	CCD <i>A</i> value
Adenylate cyclase 6	Adcy6	9.61	10.71
Adenylate cyclase 9	Adcy9	7.35	7.55
Adenylate cyclase 5	Adcy5	7.07	7.02
Guanylate cyclase 1, soluble, alpha 3	Gucy1a3	6.40	6.00
Adenylate cyclase 3	Adcy3	6.23	6.16
CD38 antigen	Cd38	6.23	5.73
Adenylate cyclase 4	Adcy4	6.17	5.85
Adenylate cyclase 7	Adcy7	6.17	6.05

Table 4 Phosphodiesterases

Gene name	Gene Symbol	DCT/CNT <i>A</i> value	CCD <i>A</i> value
Phosphodiesterase 1A, calmodulin dependent	Pde1a	10.75	10.99
Phosphodiesterase 3B, cGMP-inhibited	Pde3b	10.39	10.94
Phosphodiesterase 8A	Pde8a	10.21	10.00
Phosphodiesterase 8B	Pde8b	9.63	10.52
Phosphodiesterase 6D, cGMP-specific, rod, delta	Pde6d	8.84	9.20
Phosphodiesterase 1C	Pde1c	8.22	9.20
Phosphodiesterase 2A, cGMP-stimulated	Pde2a	7.92	7.25
Phosphodiesterase 7A	Pde7a	7.59	8.15
Phosphodiesterase 4B, cAMP specific	Pde4b	7.49	8.35
2',3'-Cyclic nucleotide 3' Phosphodiesterase	Cnp	7.43	8.10
Phosphodiesterase 7B	Pde7b	7.17	8.18
Phosphodiesterase 4A, cAMP specific	Pde4a	7.05	6.82
Phosphodiesterase 9A	Pde9a	6.78	6.97
Phosphodiesterase 6H, cGMP-specific, cone, gamma	Pde6h	6.64	6.09
Phosphodiesterase 10A	Pde10a	6.45	7.26
Phosphodiesterase 1B, Ca ²⁺ -calmodulin dependent	Pde1b	5.85	4.71 ^a

^a The *A* value is below the cutoff level

regulation of transport proteins, including the Na,K-ATPase, aqp-2, ROMK, and acid–base transporters [26–29]. The ROMK has been also shown as a substrate of tyrosine phosphatases [30]. Dual specificity phosphatases are thought to participate in renal function mainly by dephosphorylating kinases involved in the stress response (e.g., MAP kinases).

A-kinase-anchoring proteins

A-kinase-anchoring proteins (AKAPs) constitute a family of scaffold proteins involved in the targeting of protein kinase A to its substrates. The AKAPs have been extensively studied for their role in the PKA-dependent regulation of aqp-2 and ENaC activity. Henn et al. and Okutsu et al. have demonstrated that aqp-2 is colocalized with AKAP7 (AKAP18) and AKAP11 (AKAP220) in subapical vesicles of the principal cell [31, 32]. Bengrine et al. have shown that AKAP7 is also involved in the feedback inhibition of ENaC [33]. It has been proposed that these AKAPs are required for compartmentalization of cAMP signaling in the principal cell. As shown in Table 7, we found both AKAP7 and AKAP11 in the DCT/CNT and CCD transcriptomes. However, the role of the more abundant AKAPs 2, 9, and 8 has not yet been assessed.

Phospholipases

Phospholipases play important roles in transmembrane signaling processes activated by GPCRs and receptor tyrosine kinases. Receptor-mediated activation of phos-

pholipases results in hydrolysis of membrane phospholipids and generation of phospholipid-derived second messengers. PLC is a family of enzymes which catalyzes the hydrolysis of phosphatidylinositol 4,5-bisphosphate to produce diacylglycerol (DAG) and inositol 1,4,5-trisphosphate. In the DCT/CNT and/or the CCD, several targets of PLC/DAG/PKC cascade have been identified, including TRPV5 calcium channel, aqp-2, ROMK, and ENaC [34–37]. We found that the most abundant phospholipase in the DCT/CNT and the CCD is Plcg1, a PLC activated by a variety of growth factors including platelet-derived growth factor, hepatocyte growth factor, and fibroblast growth factor (Table 8). Recently, Irrazabal et al. have shown that Plcg1 contributes to the osmoprotective effect of TonEBP/OREBP transcriptional factor in the kidney [38]. Analysis of both transcriptomes also revealed expression of Ca²⁺-sensitive PLC isoforms Plcd3 and Plcd1 but only a low amount of Gq-activated Plcb1. Phospholipase A2 (PLA2) catalyzes the hydrolysis of phospholipids to generate free fatty acids and lysophospholipids. One of the principal products of PLA2 activity is the arachidonic acid, a precursor in the biosynthesis of prostaglandins and other eicosanoids. Prostaglandins are known to regulate water and solutes transport in an autocrine or paracrine manner by activating apical or basolateral GPCRs. According to our data, the principal PLA2 isoforms expressed in the DCT/CNT and the CCD are Pla2g4a, Pla2g15, and Pla2g6 (Table 8). Phospholipase D (PLD) isoforms which are also abundantly represented in both transcriptomes have been recently shown to be important regulators of endocytosis and endosomal recycling pathways [39].

Table 5 Protein kinases

Gene name	Gene Symbol	DCT/CNT <i>A</i> value	CCD <i>A</i> value
Serine/threonine kinases			
Calcium/calmodulin-dependent protein kinase II, beta	Camk2b	12.95	13.41
PCTAIRE-motif protein kinase 1	Pctk1	12.51	12.68
WNK lysine-deficient protein kinase 1	Wnk1	12.48	11.27
Proviral integration site 3	Pim3	12.43	12.20
Serum/glucocorticoid regulated kinase 1	Sgk1	11.98	12.86
Mitogen-activated protein kinase kinase kinase 12	Map3k12	11.85	11.90
MAP kinase-interacting serine/threonine kinase 2	Mknk2	11.54	12.23
p21 (CDKN1A)-activated kinase 4	Pak4	11.53	12.31
AP2-associated kinase 1	Aak1	11.50	11.93
Serum/glucocorticoid regulated kinase 2	Sgk2	11.42	10.91
TAO kinase 3	Taok3	11.34	10.85
Glycogen synthase kinase 3 beta	Gsk3b	11.28	12.04
Casein kinase 1, delta	Csnk1d	11.20	11.79
Rho-associated coiled-coil containing protein kinase 1	Rock1	11.13	11.28
Mitogen-activated protein kinase-activated protein kinase 3	Mapkapk3	11.07	11.40
NIMA (never in mitosis gene a)-related expressed kinase 7	Nek7	11.02	11.20
Casein kinase 1, alpha 1	Csnk1a1	11.01	11.56
WNK lysine-deficient protein kinase 4	Wnk4	10.99	10.46
p21 (CDKN1A)-activated kinase 2	Pak2	10.91	11.60
Pyruvate dehydrogenase kinase, isoenzyme 2	Pdk2	10.80	10.80
Nonreceptor tyrosine kinases			
Fyn-related kinase	Frk	10.1	10.91
Dual-specificity tyrosine-(Y)-phosphorylation regulated kinase 1a	Dyrk1a	9.55	10.59
PTK2 protein tyrosine kinase 2	Ptk2	9.15	10.02
PTK2 protein tyrosine kinase 2 beta	Ptk2b	8.81	8.85
Lemur tyrosine kinase 2	Lmtk2	8.73	9.99
Fer (fms/fps-related) protein kinase, testis specific 2	Fert2	8.73	9.47
Janus kinase 2	Jak2	8.66	9.12
Janus kinase 1	Jak1	8.46	9.24
Tyrosine kinase, nonreceptor, 1	Tnk1	8.25	8.78
FMS-like tyrosine kinase 1	Flt1	8.24	7.46
FMS-like tyrosine kinase 4	Flt4	8.18	7.82
Tyrosine kinase, non-receptor, 2	Tnk2	7.83	8.34
Tec protein tyrosine kinase	Tec	7.76	7.94
Tyrosine kinase 2	Tyk2	7.18	7.53
c-Mer proto-oncogene tyrosine kinase	Mertk	7.12	6.24
c-Src tyrosine kinase	Csk	7.02	7.59
Serine/threonine/tyrosine kinase 1	Styk1	6.99	8.85
PTK7 protein tyrosine kinase 7	Ptk7	6.53	6.49
Aatyk3 mRNA for apoptosis-associated tyrosine kinase 3	Lmtk3	6.29	6.04
Tyrosine kinase receptors			
Met proto-oncogene	Met	11.36	11.87
Discoidin domain receptor family, member 1 receptor	Ddr1	11.35	11.45
Fibroblast growth factor receptor 2	Fgfr2	10.31	11.30
Insulin receptor	Insr	9.52	9.83
Insulin receptor-related receptor	Insrr	9.50	10.06
Insulin-like growth factor I receptor	Igf1r	9.04	9.99

Table 5 (continued)

Gene name	Gene Symbol	DCT/CNT <i>A</i> value	CCD <i>A</i> value
Endothelial-specific receptor tyrosine kinase	Tek	8.85	9.32
Fibroblast growth factor receptor 1	Fgfr1	8.82	8.93
Eph receptor B4	Ephb4	8.63	8.87
Receptor-like tyrosine kinase	Ryk	8.21	8.45
Eph receptor A1	Epha1	7.37	7.72
Eph receptor B2	Ephb2	7.14	7.07
Fibroblast growth factor receptor 3	Fgfr3	7.04	7.03
Epidermal growth factor receptor	Egfr	7.01	8.54
Tyrosine kinase with immunoglobulin-like and EGF-like domains 1	Tie1	6.91	6.73
Eph receptor B3	Ephb3	6.63	6.11
c-Abl oncogene 1, receptor tyrosine kinase	Abl1	6.62	7.24
AXL receptor tyrosine kinase	Axl	6.23	5.93
Receptor tyrosine kinase-like orphan receptor 1	Ror1	5.84	6.21
Eph receptor A4	Epha4	5.74 ^a	6.31

^a The *A* value is below the cutoff level

Small GTP-binding proteins

Small GTP-binding proteins are low molecular weight GTPases (20–25 kDa) that control a variety of cellular processes including vesicle transport, cytoskeleton dynamics, cell division, and immune response. All small GTPases can be divided in five subfamilies, namely the Rab subfamily, the ADP-ribosylating factor (Arf) subfamily, the Rho/Rac/Cdc42 subfamily, the Ras/Ral/Rap subfamily, and the Ran GTPase. More than 50 members of the Rab subfamily were found to be expressed at significant levels (Table 9 and Supplemental Table 4). The members of this family are implicated in the transport, docking, and fusion of endocytotic vesicles. Van de Graaf et al. have shown that Rab11a is required for the intracellular trafficking of TRPV5 and TRPV6 calcium channels to the cell surface [40]. Curtis and Gluck have demonstrated that Rab11 and Rab20 are mainly expressed in V-ATPase expressing intercalated cells of the collecting duct, whereas principal cells of the collecting duct and of the distal nephron are enriched in Rab18 and Rab5a [41]. Several evidences indicate that Rab(s) could be involved in trafficking of CFTR, ENaC, and aqp-2 [42]. However, functional role of many highly abundant Rab(s) in DCT/CNT and CCD remains unknown. Arfs are participating in the formation of coated transport vesicles. El-Annan et al. have shown abundant expression of Arf1 and Arf6 in the distal nephron and the collecting duct and have demonstrated that Arf1 is mostly localized to the apical membrane whereas Arf6 appeared to be mainly expressed at the basolateral membrane [43]. Arf6 was further demonstrated as a factor promoting Avpr2 recycling [44]. Our data confirm high

expression levels of Arf1 and Arf6 and reveal abundant expression of several Arfs (Arf3, Arl1, Arl3, etc., see Table 9) with yet unassigned function in the renal tubule. As shown in Table 9, both the DCT/CNT and the CCD also exhibit high expression levels of several Rho GTPases, including Cdc42, RhoA, and Rac1. The main function of Rho GTPases consists in the control of cytoskeleton dynamics and assembly. Thus, it was logically proposed that Rho(s) could be involved in trafficking of aqp-2, a process which requires remodeling of microtubules and filaments. However, evidence that support this hypothesis remains limited to a few in vitro studies [45, 46]. Members of Ras subfamily share the highest degree of homology with Ras, one of the most frequently mutated oncogenes in cancer. Ras, Ral, and Rap have been shown to play an important role in cellular proliferation and differentiation by influencing a number of intracellular signaling pathways. Ras GTPases have been also shown to influence activity or expression of several important DCT/CNT and/or CCD transporters, including NCC (H-ras), H,K-ATPase (Rap1), ENaC (K-ras), and aqp-2 (Rap1) [47–50]. As shown in Table 9, H-ras, K-ras, and Rap1 are present within the ten most abundant members of the Ras subfamily. However, the role of several other highly abundant Ras GTPases, including the most abundant Rragd, remains unknown.

SNAREs and SNARE-related proteins

SNARE proteins participate in the trafficking of renal transporters by mediating fusion of intracellular vesicles to the target membranes. Molecular composition of SNARE complexes has been extensively studied for aquaporins

Table 6 Protein phosphatases

Gene name	Gene Symbol	DCT/CNT A value	CCD A value
Serine/threonine phosphatases			
Protein phosphatase 2 (formerly 2A), alpha isoform	Ppp2r1a	12.51	12.72
Protein phosphatase 1, catalytic subunit, gamma isoform	Ppp1cc	11.76	12.14
Protein phosphatase 1, catalytic subunit, beta isoform	Ppp1cb	11.35	11.90
Protein phosphatase 1, catalytic subunit, alpha isoform	Ppp1ca	11.17	11.79
Protein phosphatase 1B, magnesium dependent, beta isoform	Ppm1b	11.15	11.49
Protein phosphatase 1H (PP2C domain containing)	Ppm1h	10.87	11.35
Protein phosphatase 2, alpha isoform	Ppp2r5a	10.85	11.19
Protein phosphatase 2 (formerly 2A), catalytic subunit, alpha	Ppp2ca	10.68	10.96
PTC7 protein phosphatase homolog (<i>S. cerevisiae</i>)	Pptc7	10.37	10.32
Protein phosphatase 1A, magnesium dependent, alpha isoform	Ppm1a	10.20	10.66
Protein phosphatase 1K (PP2C domain containing)	Ppm1k	10.13	10.67
Protein phosphatase 2, epsilon isoform	Ppp2r5e	9.82	10.29
Protein phosphatase 2 (formerly 2A), alpha isoform	Ppp2r2a	9.80	10.36
Protein phosphatase 2, gamma isoform	Ppp2r5c	9.55	10.18
Protein phosphatase 6, catalytic subunit	Ppp6c	9.55	9.76
Protein phosphatase 2, regulatory subunit B, delta isoform	Ppp2r2d	9.44	9.41
Protein phosphatase 3, catalytic subunit, alpha isoform	Ppp3ca	9.41	9.52
Protein phosphatase 1G, magnesium dependent, gamma isoform	Ppm1g	9.37	10.02
Protein phosphatase 2 (formerly 2A), beta isoform	Ppp2r1b	9.25	9.58
Protein phosphatase 5, catalytic subunit	Ppp5c	9.19	9.30
Tyrosine phosphatases			
Acid phosphatase 1, soluble	Acp1	12.20	12.28
Protein tyrosine phosphatase 4a2	Ptp4a2	11.67	12.30
Protein tyrosine phosphatase, receptor type, F	Ptprf	10.74	11.32
Protein tyrosine phosphatase, receptor type, J	PtpRJ	10.60	11.51
Protein tyrosine phosphatase, non-receptor type 11	Ptpn11	10.44	10.73
Protein tyrosine phosphatase, receptor type, S	PtpRS	10.26	10.29
Protein tyrosine phosphatase, non-receptor type 1	Ptpn1	9.40	9.53
Protein tyrosine phosphatase, non-receptor type 2	Ptpn2	9.26	9.67
Protein tyrosine phosphatase, receptor type, K	PtpRK	9.11	9.22
Protein tyrosine phosphatase, receptor type, A	PtpRA	8.96	9.64
Protein tyrosine phosphatase, non-receptor type 9	Ptpn9	8.95	9.38
Protein tyrosine phosphatase, mitochondrial 1	Ptpmt1	8.88	8.98
Protein tyrosine phosphatase, non-receptor type 13	Ptpn13	8.83	9.61
Protein tyrosine phosphatase, non-receptor type 14	Ptpn14	8.75	9.59
Similar to protein tyrosine phosphatase, receptor type, G	PtpRG	8.53	7.55
Protein tyrosine phosphatase, receptor type, D	PtpRD	8.48	8.11
Protein tyrosine phosphatase, receptor type, C	PtpRC	8.36	8.46
Protein tyrosine phosphatase, receptor type, M	PtpRM	8.36	8.97
Protein tyrosine phosphatase, non-receptor type 21	Ptpn21	8.13	8.83
Protein tyrosine phosphatase, receptor type, G	PtpRG	7.91	8.01
Dual-specificity phosphatases			
Dual specificity phosphatase 1	Dusp1	11.46	11.73
Dual specificity phosphatase 3	Dusp3	10.47	10.92
Slingshot homolog 1 (<i>Drosophila</i>)	Ssh1	9.19	9.73
Dual specificity phosphatase 16	Dusp16	8.91	9.64
CDC14 cell division cycle 14 homolog A (<i>S. cerevisiae</i>)	Cdc14a	8.68	9.04

Table 6 (continued)

Gene name	Gene Symbol	DCT/CNT <i>A</i> value	CCD <i>A</i> value
Dual specificity phosphatase 19	Dusp19	8.40	9.32
Dual specificity phosphatase 22	Dusp22	8.02	8.08
Dual specificity phosphatase 6	Dusp6	7.69	7.86
Dual specificity phosphatase 7	Dusp7	7.49	8.11
CDC14 cell division cycle 14 homolog B (<i>S. cerevisiae</i>)	Cdc14b	7.41	8.17
Dual specificity phosphatase 23	Dusp23	7.40	7.18
Dual specificity phosphatase 26 (putative)	Dusp26	7.30	6.08
Dual specificity phosphatase 12	Dusp12	7.28	7.84
Slingshot homolog 2 (<i>Drosophila</i>)	Ssh2	7.06	7.57
Dual specificity phosphatase 28	Dusp28	7.04	7.04
Dual specificity phosphatase 18	Dusp18	6.92	6.69
Slingshot homolog 2 (<i>Drosophila</i>)	Ssh2	6.58	7.73
Dual specificity phosphatase 8	Dusp8	6.41	6.54
Slingshot homolog 3 (<i>Drosophila</i>)	Ssh3	6.39	6.72
Dual specificity phosphatase 4	Dusp4	6.28	5.61 ^a

^a The *A* value is below the cutoff level

involved in renal urine concentration mechanism. Mistry et al. have shown that aqp-2 sorting to the apical membrane requires snapin (SNAPAP), SNAP23, and syntaxin-3, whereas syntaxin-4 is preferentially involved in cell surface expression of aqp-3 [51]. SNAP23/syntaxin-1a complex has been also proposed to regulate cell surface expression of ENaC. However, in our data, expression levels of syntaxin-1a are low (*A* values of 4.7 and 5.0 in the DCT/CNT and the CCD, respectively). Accordingly, only a low signal intensity for syntaxin-1a was detected in the IMCD hybridization data [11]. As shown in Table 10 and Supplemental Table 5, both the DCT/CNT and the CCD exhibit high expression of SNAPAP, SNAP23, syntaxin-3, and syntaxin-4. High expression levels were also detected

for vesicle-associated membrane proteins (VAMP) 2, 8, and 3. VAMP2 and VAMP3 proteins were previously identified in aqp-2-containing intracellular vesicles, indicating their involvement in aqp-2 trafficking [52]. Recently, Wang et al. have shown that mice devoid of *VAMP8* gene exhibit a diabetes-insipidus-like phenotype and a significantly reduced membrane expression of aqp-2 in collecting duct cells [53].

Clathrin, clathrin adaptors, and dynamin-like GTPases

Clathrin-coated vesicles are major protein carriers in protein endocytotic pathways. Clathrin-coated vesicles mediate endocytosis of many essential DCT/CNT and/or CCD

Table 7 A kinase anchor proteins

Gene name	Gene Symbol	DCT/CNT <i>A</i> value	CCD <i>A</i> value
A kinase (PRKA) anchor protein 2	Akap2	11.85	11.85
A kinase (PRKA) anchor protein (yotiao) 9	Akap9	10.32	10.55
A kinase (PRKA) anchor protein 8	Akap8	9.41	9.93
A kinase (PRKA) anchor protein 11	Akap11	8.42	8.69
A kinase (PRKA) anchor protein 1	Akap1	8.26	8.75
A kinase (PRKA) anchor protein 13	Akap13	7.76	8.55
A kinase (PRKA) anchor protein (gravin) 12	Akap12	7.42	7.39
A kinase (PRKA) anchor protein 10	Akap10	7.20	6.94
A kinase (PRKA) anchor protein 8-like	Akap8l	7.11	8.33
A kinase (PRKA) anchor protein 7	Akap7	6.92	8.25
A kinase (PRKA) anchor protein 3	Akap3	6.66	6.45
A kinase (PRKA) anchor protein 6	Akap6	5.99	5.23 ^a
A kinase (PRKA) anchor protein 14	Akap14	5.97	5.79 ^a

^a The *A* value is below the cutoff level

Table 8 Phospholipases

Gene name	Gene Symbol	DCT/CNT <i>A</i> value	CCD <i>A</i> value
Phospholipase C, gamma 1	Plcg1	10.39	10.38
Lysophospholipase 1	Lypla1	9.73	9.63
Patatin-like phospholipase domain containing 2	Pnpla2	8.97	9.60
Sec23 interacting protein	Sec23ip	8.65	9.10
Lysophospholipase-like 1	Lyplal1	8.55	9.04
DDHD domain containing 2	Ddhd2	8.54	9.49
Phospholipase D family, member 3	Pld3	8.44	8.82
Lysophospholipase 2	Lypla2	8.41	7.38
Phospholipase A2, group IVA (cytosolic, calcium-dependent)	Pla2g4a	8.26	9.35
Phospholipase C, delta 3	Plcd3	8.18	9.23
Preimplantation protein 4	Prei4	7.89	8.17
Phospholipase A2, group XV	Pla2g15	7.62	8.25
Phospholipase C, delta 4	Plcd4	7.04	6.68
DDHD domain containing 1	Ddhd1	6.87	7.65
Phospholipase A2, group VI	Pla2g6	6.77	6.30
Phospholipase D2	Pld2	6.67	7.04
Phospholipase C, beta 1	Plcb1	6.25	6.00
Phospholipase C, delta 1	Plcd1	6.25	7.15

transporting proteins including ROMK, Na,K-ATPase, ENaC, aqp-2, and Trpv5 [54–58]. As shown in Table 11, both the DCT/CNT and the CCD exhibit high expression levels of clathrin light and heavy chains (Clta, Cltb, and Cltc, respectively) as well as several clathrin adaptor subunits (Ap1s3, Ap2s1, and Ap3s1). Similar to the IMCD [11], our data show a high abundance of Picalm, a clathrin adaptor which was recently shown to direct VAMP2 trafficking during endocytosis [59]. Dynamins are high molecular weight GTPases (~100 kDa) that mediate the fission of clathrin-coated vesicles from the membrane. As shown in Table 11, both transcriptomes reveal a high expression of dynamin 2 (Dnm2) and dynamin 1-like (Dnm1) and low expression of dynamins 1 and 3 (Dnm1 and Dnm3, respectively). Interestingly, this distribution of dynamins differs significantly from that of IMCD in which only dynamin-like GTPases Mx1 and Mx2 demonstrated high signal intensities [11]. In the DCT/CNT and the CCD transcriptomes, both Mx1 and Mx2 exhibit low expression levels (Mx1: *A* values of 4.3 and 3.8 in DCT/CNT and CCD, respectively; Mx2: *A* values of 3.5 and 3.0 in DCT/CNT and CCD, respectively).

Cytoskeletal proteins and cytoskeletal regulators

Cytoskeletal proteins mediate a wide variety of essential renal functions. During fetal kidney development, the assembly and contraction of microtubules and microfilaments have been proposed as part of a mechanism that drives branching morphogenesis of the ureteric bud [60]. In

the adult kidney, cytoskeleton remodeling has been shown to influence cell surface expression and/or activity of a number of proteins involved in maintaining balance of water and electrolytes, including ENaC, aqp-2, Na,K-ATPase, secretory K channels, and chloride channels [61–65]. A significant number of cytoskeletal proteins have been recently identified by a proteomic approach in the aqp-2-containing vesicles in the IMCD [52]. As shown in Table 12 and Supplemental Table 6, ~300 different transcripts encoding cytoskeletal and cytoskeletal-related proteins are present in our data. The overall distribution and abundance of cytoskeletal transcripts in the DCT/CNT and the CCD are largely similar to that identified in the IMCD. However, for several major transcripts, a significant difference was observed. For instance, moesin, an actin-binding protein which has been shown to modulate activity of aqp-2, Na,K-ATPase, and CFTR in different models of epithelial cells, was undetectable in IMCD transcriptome [11, 66–68]. In our study, moesin is abundantly present in both the DCT/CNT and the CCD (see subcategory *actin and actin-binding proteins*, Table 12). Also, our data reveal high expression of myosin VI (Myo6), a myosin which has been shown as a prerequisite for the clathrin-dependent endocytosis of CFTR in the intestine [69] (see subcategory *myosin and myosin-like proteins*, Table 12). The role of Myo6 in the kidney has not yet been investigated. In subcategory *microtubule and microtubule-related proteins* (Table 12), we found strong expression of tubulins 1b and 1a (Tuba1b and Tuba1a), two tubulins that were not detected in the IMCD. Again, despite a high abundance of

Table 9 Small GTPases

Gene name	Gene Symbol	DCT/CNT <i>A</i> value	CCD <i>A</i> value
Rab small GTP-binding proteins			
RAB1, member RAS oncogene family	Rab1	12.58	12.82
RAB14, member RAS oncogene family	Rab14	11.96	12.08
RAB7, member RAS oncogene family	Rab7	11.69	12.07
RAB10, member RAS oncogene family	Rab10	11.68	11.85
RAB2A, member RAS oncogene family	Rab2a	11.67	11.90
RAB21, member RAS oncogene family	Rab21	11.29	11.53
RAB18, member RAS oncogene family	Rab18	10.68	11.30
RAB11a, member RAS oncogene family	Rab11a	10.44	10.77
RAB28, member RAS oncogene family	Rab28	10.41	11.10
RAB22A, member RAS oncogene family	Rab22a	10.23	10.42
RAB9, member RAS oncogene family	Rab9	9.98	10.24
RAB4A, member RAS oncogene family	Rab4a	9.94	10.23
RAB11B, member RAS oncogene family	Rab11b	9.83	10.88
RAB17, member RAS oncogene family	Rab17	9.74	10.19
RAB6B, member RAS oncogene family	Rab6b	9.73	10.27
RAB25, member RAS oncogene family	Rab25	9.61	10.31
RAB6, member RAS oncogene family	Rab6	9.60	9.96
RAB20, member RAS oncogene family	Rab20	9.54	10.82
RAB5A, member RAS oncogene family	Rab5a	9.48	10.06
RAB5B, member RAS oncogene family	Rab5b	9.46	10.01
Arf small GTP-binding proteins			
ADP-ribosylation factor 6	Arf6	12.58	13.00
ADP-ribosylation factor 1	Arf1	11.89	11.93
ADP-ribosylation factor 3	Arf3	11.64	12.25
ADP-ribosylation factor-like 1	Arl1	11.61	11.94
ADP-ribosylation factor-like 3	Arl3	11.46	11.73
SAR1 gene homolog A (<i>S. cerevisiae</i>)	Sar1a	11.46	12.09
SAR1 gene homolog B (<i>S. cerevisiae</i>)	Sar1b	10.69	11.12
ADP-ribosylation factor 4	Arf4	10.48	10.99
ADP-ribosylation factor-like 4C	Arl4c	10.07	9.25
ADP-ribosylation factor-like 5A	Arl5a	9.72	10.22
ADP-ribosylation factor-like 8B	Arl8b	9.53	10.18
ADP-ribosylation factor-like 4A	Arl4a	9.18	9.27
ADP-ribosylation factor related protein 1	Arfip1	9.05	9.73
ADP-ribosylation factor-like 6	Arl6	8.90	9.54
ADP-ribosylation factor-like 8A	Arl8a	8.87	9.33
ADP-ribosylation factor 2	Arf2	8.52	9.15
ADP-ribosylation factor-like 2	Arl2	7.85	8.20
ADP-ribosylation factor-like 4D	Arl4d	7.38	9.24
ADP-ribosylation factor-like 5B	Arl5b	7.17	7.52
Tripartite motif-containing 23	Trim23	6.07	6.90
Rho small GTP-binding proteins			
Cell division cycle 42 homolog (<i>S. cerevisiae</i>)	Cdc42	12.89	12.74
Ras homolog gene family, member A	Rhoa	11.66	11.84
RAS-related C3 botulinum substrate 1	Rac1	11.32	11.81
Ras homolog gene family, member B	Rhob	9.80	10.14
Ras homolog gene family, member U	Rhou	9.77	10.58

Table 9 (continued)

Gene name	Gene Symbol	DCT/CNT <i>A</i> value	CCD <i>A</i> value
Ras homolog gene family, member Q	Rhoq	8.74	9.34
Rho family GTPase 3	Rnd3	8.16	9.13
Ras homolog gene family, member T2	Rhot2	8.06	8.88
Ras homolog gene family, member T1	Rhot1	8.05	8.84
Rho-related BTB domain containing 1	Rhobtb1	7.44	8.02
Rho-related BTB domain containing 2	Rhobtb2	7.39	7.54
Ras homolog gene family, member C	Rhoc	7.35	8.05
Rho family GTPase 2	Rnd2	7.18	7.67
Ras homolog gene family, member D	Rhod	6.74	7.87
Ras homolog gene family, member J	Rhoj	6.70	6.50
Rho-related BTB domain containing 3	Rhobtb3	6.63	7.56
Ras homolog gene family, member G	Rhog	5.83	6.67
RAS-related C3 Botulinum substrate 3	Rac3	5.71 ^a	6.03
Ras and Ras-related small GTP-binding proteins			
Ras-related GTP binding D	Rragd	12.40	12.60
RAS-related protein 1b	Rap1b	10.75	11.28
RAS-related protein-1a	Rap1a	10.33	10.80
v-Ki-ras2 Kirsten rat sarcoma viral oncogene homolog	K-ras	10.32	10.57
RAN, member RAS oncogene family	Ran	9.81	10.39
V-ral simian leukemia viral oncogene homolog A (ras-related)	Rala	9.34	9.79
Harvey rat sarcoma virus oncogene 1	Hras1	9.18	9.21
Ras-related GTP binding C	Rragc	9.14	9.67
v-ral simian leukemia viral oncogene homolog B (ras-related)	Ralb	9.08	10.30
Neuroblastoma ras oncogene	Nras	9.02	9.38
NFKB inhibitor interacting Ras-like protein 1	Nkiras1	8.78	9.10
Ras-related GTP binding A	Rraga	8.50	8.68
RAS-related protein 2a	Rap2a	8.24	8.82
RAP2B, member of RAS oncogene family	Rap2b	8.20	9.23
Harvey rat sarcoma oncogene, subgroup R	Rras	8.04	8.51
Ras-like without CAAX 1	Rit1	7.79	8.31
RAS-like, family 11, member B	Rasl11b	7.73	9.02
Muscle and microspikes RAS	Mras	7.64	7.79
NFKB inhibitor interacting Ras-like protein 2	Nkiras2	7.60	7.79
RAS, dexamethasone-induced 1	Rasd1	7.40	7.76

^a The *A* value is below the cutoff level

these transcripts, their role in the kidney remains unknown. Finally, in subcategory *intermediate filaments and related proteins* (Table 12), we detected several keratins not present in the IMCD transcriptome (Krt10, Krt80, Krt23, and Krt34).

Transporters and channels

As shown in Table 13 and Supplemental Table 7, more than 250 transcripts encoding water/solute-transporting proteins are expressed at significant levels in the DCT/CNT and/or the CCD, confirming the variety of solutes transported

across the epithelium of these segments. In subcategory *water channels* (Table 13), aquaporins are abundantly represented by plasma membrane expressed aquaporins 2, 3, and 4, as well as by the intracellular aquaporins 6 and 11. As expected, expression of aquaporins 2 and 4 is significantly lower in the DCT/CNT than in the CCD, whereas aquaporin-3 is equally represented in both transcriptomes. Surprisingly, our analysis also revealed a low, but significant, expression of aquaporin 1, a channel which is present, according to immunohistochemical analyses, only in the proximal tubule and descending thin limb. Interestingly, the aquaporin 1 RNA has also been detected

Table 10 SNAREs

Gene name	Gene Symbol	DCT/CNT <i>A</i> value	CCD <i>A</i> value
Vesicle-associated membrane protein 2	Vamp2	11.74	11.38
Vesicle-associated membrane protein 8	Vamp8	11.66	12.03
Synaptosomal-associated protein 23	Snap23	11.50	11.72
Synaptosomal-associated protein, 47	Snap47	11.19	11.51
Vesicle transport through interaction with t-SNAREs 1B homolog	Vti1b	10.68	10.94
Syntaxin 7	Stx7	10.64	11.30
Vesicle-associated membrane protein 3	Vamp3	10.55	10.89
Syntaxin 8	Stx8	10.40	11.16
SNAP-associated protein	Snapap	10.18	10.61
YKT6 homolog (<i>S. cerevisiae</i>)	Ykt6	9.73	10.37
Syntaxin 3	Stx3	9.60	10.30
Syntaxin 4A (placental)	Stx4a	9.49	9.99
Syntaxin 12	Stx12	9.47	10.30
Blocked early in transport 1 homolog (<i>S. cerevisiae</i>)-like	Bet11	9.38	9.35
Golgi SNAP receptor complex member 1	Gosr1	9.37	9.75
SEC22 vesicle trafficking protein homolog B (<i>S. cerevisiae</i>)	Sec22b	9.35	9.73
Syntaxin 16	Stx16	9.04	9.23
Blocked early in transport 1 homolog (<i>S. cerevisiae</i>)	Bet1	9.02	9.64
Golgi SNAP receptor complex member 2	Gosr2	8.85	8.65
Vesicle-associated membrane protein 4	Vamp4	8.63	8.80

Table 11 Vesicle coat proteins

Gene name	Gene Symbol	DCT/CNT <i>A</i> value	CCD <i>A</i> value
Clathrin and clathrin adaptors			
Clathrin, light polypeptide (Lca)	Clta	12.71	12.90
Synaptophysin-like protein	Syp1	11.60	12.02
Clathrin, light polypeptide (Lcb)	Cltb	10.56	10.87
Clathrin, heavy polypeptide (Hc)	Cltc	10.38	10.96
Phosphatidylinositol binding clathrin assembly protein	Picalm	10.16	10.89
Adaptor-related protein complex AP-1, sigma 3	Ap1s3	9.49	10.48
Adaptor-related protein complex 2, sigma 1 subunit	Ap2s1	9.07	10.26
Adaptor-related protein complex 3, sigma 1 subunit	Ap3s1	9.04	9.48
Epsin 2	Epn2	8.41	9.24
Adaptor protein complex AP-1, sigma 1	Ap1s1	8.19	8.50
Adaptor-related protein complex AP-4, sigma 1	Ap4s1	7.82	8.06
Adaptor-related protein complex 3, sigma 2 subunit	Ap3s2	7.80	8.59
Epsin 1	Epn1	7.47	7.11
Adaptor-related protein complex 1, sigma 2 subunit	Ap1s2	6.62	6.15
Epsin 3	Epn3	6.19	6.81
Synaptosomal-associated protein 91	Snap91	6.14	5.14 ^a
Dynamin-like GTPases			
Dynamin 2	Dnm2	10.71	11.22
Dynamin 1-like	Dnm11	10.18	10.8
Dynamin 1	Dnm1	5.98	5.82
Dynamin 3	Dnm3	5.79 ^a	7.39

^a The *A* value is below the cutoff level

Table 12 Cytoskeleton and cytoskeleton-related proteins

Gene name	Gene Symbol	DCT/CNT <i>A</i> value	CCD <i>A</i> value
Actin and actin-binding proteins			
Actin, beta	Actb	13.35	13.80
Cofilin 1, nonmuscle	Cfl1	12.96	12.98
Actin, gamma, cytoplasmic 1	Actg1	12.93	13.06
Catenin (cadherin-associated protein), beta 1	Ctnnb1	12.74	13.26
Syndecan 4	Sdc4	12.61	12.99
Catenin (cadherin-associated protein), alpha 1	Ctnna1	12.59	13.02
Tropomyosin 1, alpha	Tpm1	12.30	12.87
Wiskott-Aldrich syndrome-like (human)	Wasl	11.90	12.81
Spectrin beta 2	Spnb2	11.76	12.23
LIM and SH3 protein 1	Lasp1	11.67	11.83
Cingulin-like 1	Cgnl1	11.56	12.13
ARP2 actin-related protein 2 homolog (yeast)	Actr2	11.49	12.01
Tensin 1	Tns1	11.47	11.85
Gelsolin	Gsn	11.37	12.06
Cortactin	Cttn	11.33	12.17
Cysteine and glycine-rich protein 1	Csrp1	11.18	11.75
Cofilin 2, muscle	Cfl2	11.13	11.49
Utrophin	Utm	11.12	12.18
Radixin	Rdx	11.11	11.24
Tensin 3	Tns3	11.03	11.71
Myosin and myosin-like proteins			
Myosin, heavy polypeptide 9, nonmuscle	Myh9	12.12	12.56
Myosin, light chain 12B, regulatory	Myl12b	11.80	12.55
Myosin X	Myo10	10.70	10.60
Myosin IC	Myo1c	10.64	10.58
Myosin VI	Myo6	10.21	10.93
Myosin, heavy polypeptide 10, nonmuscle	Myh10	10.14	11.43
Myosin 1H	Myo1h	9.23	10.17
Myosin XVIII A	Myo18a	9.14	9.71
Myosin VB	Myo5b	8.56	9.06
Myosin IXb	Myo9b	8.52	9.12
Myosin IE	Myo1e	8.32	8.95
Myosin, light polypeptide 9, regulatory	Myl9	8.26	6.85
Myosin ID	Myo1d	7.95	8.73
Myosin IXa	Myo9a	7.89	8.72
Myosin VA	Myo5a	7.87	7.97
Myosin VC	Myo5c	7.64	8.70
Myosin, heavy polypeptide 11, smooth muscle	Myh11	7.43	5.61 ^a
Myosin, heavy polypeptide 6, cardiac muscle, alpha	Myh6	6.85	6.53
Myosin, heavy polypeptide 7, cardiac muscle, beta	Myh7	6.84	6.57
Myosin VII B	Myo7b	6.75	6.47
Microtubule and microtubule-related proteins			
Tubulin, alpha 4A	Tuba4a	13.63	13.51
Tubulin, alpha 1B	Tuba1b	12.88	13.17
Tubulin, alpha 1A	Tuba1a	12.61	12.89
Tubulin, beta 2A	Tubb2a	12.32	12.64
Gamma-aminobutyric acid (GABA-A) receptor-associated protein-like 1	Gabarap11	12.28	12.39

Table 12 (continued)

Gene name	Gene Symbol	DCT/CNT <i>A</i> value	CCD <i>A</i> value
Microtubule-associated protein 1 light chain 3 beta	Map1lc3b	11.89	12.01
Dynein light chain roadblock-type 1	Dynlrb1	11.87	11.89
Dynein light chain LC8-type 1	Dynll1	11.86	12.45
Dynein light chain LC8-type 1 /// predicted gene, EG627788	Dynll1	11.75	12.50
Gamma-aminobutyric acid receptor-associated protein	Gabarap	11.50	11.62
Dynein light chain Tctex-type 3	Dynlt3	11.49	11.85
Dynein light chain LC8-type 2	Dynll2	11.17	11.69
Tubulin, beta 2B	Tubb2b	11.03	11.27
Kinesin family member 5B	Kif5b	11.00	11.06
Microtubule-associated protein, RP/EB family, member 1	Mapre1	10.77	11.28
Dynactin 6	Dctn6	10.76	11.35
Tubulin folding cofactor B	Tbcb	10.62	11.38
Dynactin 4	Dctn4	10.58	11.20
Kinesin family member 13B	Kif13b	10.53	10.89
Dynein cytoplasmic 1 intermediate chain 2	Dync1i2	10.36	10.55
Intermediate filaments and related proteins			
Keratin 7	Krt7	12.42	12.89
Plakophilin 4	Pkp4	11.75	11.73
Keratin 18	Krt18	11.13	12.45
Keratin 8	Krt8	10.92	11.84
Lamin A	Lmna	10.68	10.75
Plastin 3 (T-isoform)	Pls3	10.38	11.37
Plakophilin 2	Pkp2	9.51	10.12
Keratin 10	Krt10	9.39	9.68
Keratin 80	Krt80	8.25	8.54
Vimentin	Vim	8.17	7.54
Keratin 23	Krt23	7.98	9.95
Lamin B2	Lmnb2	7.07	7.40
Keratin 24	Krt24	6.95	6.00
Lamin B1	Lmnb1	6.95	7.02
Keratin 34	Krt34	6.72	6.52
Keratin 19	Krt19	6.64	7.51
Plakophilin 3	Pkp3	6.36	6.71
Plastin 1 (I-isoform)	Pls1	6.10	6.00

^a The *A* value is below the cutoff level

in human DCT, at levels of ~10% of those in the proximal tubule [70]. However, in both human and mouse transcriptomes, the expression levels of aquaporin 1 RNA in the distal nephron are significantly lower than those of other water channels. For instance, in mouse DCT/CNT, the difference between the aquaporin 3 and aquaporin 1 RNA expression is ~130-fold (13.11 units of *A* value vs. 6.09 units of *A* value, respectively, Table 13).

In subcategory *ion channels and transporters excluding solute carrier protein (SLC; Table 13)*, all principal genes involved in maintaining ion balance are represented (e.g., Na,K-ATPase, $\alpha\beta\gamma$ ENaC (Scnn1), ROMK (Kcnj1), Kir5.1

(Kcnj16), Kir 4.1 (Kcnj10), Clcnkb, Clc3, Trpv5, PMCA2 (ATP2b2), Trpm6, and various H⁺-ATPases). Analysis of the transcripts belonging to this subcategory also revealed a number of highly abundant transcripts with yet unassigned function in the kidney. For instance, both the DCT/CNT and the CCD exhibit high expression levels of Tmem16f, a functionally uncharacterized paralog of a recently identified calcium-activated chloride channel Tmem16a [71]. Also, both transcriptomes reveal abundant expression of several voltage-gated ion channels, including Kcnq1, Kcne1, Kcnj10, Cacna1d, Cacna4, Kcnh3, and Cacna2d1. Importantly, mutations in two voltage-gated potassium channels

Table 13 Transporters and channels

Gene name	Gene Symbol	DCT/CNT <i>A</i> value	CCD <i>A</i> value
Water channels			
Aquaporin 3	Aqp3	13.11	13.45
Aquaporin 6	Aqp6	11.53	12.84
Aquaporin 4	Aqp4	8.16	11.63
Aquaporin 11	Aqp11	8.11	6.90
Aquaporin 2	Aqp2	7.95	10.25
Aquaporin 5	Aqp5	6.51	6.20
Aquaporin 1	Aqp1	6.09	6.57
Ion channels and transporters excluding SLC proteins			
ATPase, Na ⁺ /K ⁺ transporting, beta 1 polypeptide	Atp1b1	13.86	13.87
Voltage-dependent anion channel 1	Vdac1	13.73	13.74
ATPase, H ⁺ transporting, lysosomal V1 subunit A	Atp6v1a	13.11	13.10
ATPase, H ⁺ transporting, lysosomal V0 subunit C	Atp6v0c	12.99	12.66
ATPase, H ⁺ transporting, lysosomal V1 subunit D	Atp6v1d	12.99	13.17
ATPase, Na ⁺ /K ⁺ transporting, alpha 1 polypeptide	Atp1a1	12.76	12.12
V-ATPase, H ⁺ transporting, lysosomal V1 subunit E1	Atp6v1e1	12.71	12.61
ATPase, H ⁺ transporting, lysosomal V0 subunit D2	Atp6v0d2	12.58	12.78
Voltage-dependent anion channel 2	Vdac2	12.54	12.63
Potassium inwardly rectifying channel, subfamily J, member 16	Kcnj16	12.44	12.63
Potassium inwardly rectifying channel, subfamily J, member 1	Kcnj1	12.41	12.69
FXYP domain-containing ion transport regulator 2	Fxyd2	12.40	11.11
ATPase, H ⁺ transporting, lysosomal V1 subunit F	Atp6v1f	12.25	12.36
ATPase, H ⁺ transporting, lysosomal V0 subunit B	Atp6v0b	12.01	11.93
ATPase, H ⁺ transporting, lysosomal V0 subunit E	Atp6v0e	11.90	11.97
Sodium channel, non-voltage-gated 1 gamma	Scnn1g	11.54	11.88
Potassium voltage-gated channel, subfamily Q, member 1	Kcnq1	11.51	11.68
Potassium voltage-gated channel, Isk-related subfamily, member 1	Kcne1	11.47	11.68
ATPase, Ca ⁺⁺ transporting, cardiac muscle, slow twitch 2	Atp2a2	11.45	11.61
Chloride channel Kb	Clcnkb	11.33	11.70
SLC			
Solute carrier family 26, member 4 (pendrin)	Slc26a4	13.43	13.45
Solute carrier family 25 (mitochondrial carrier, adenine nucleotide translocator), member 5	Slc25a5	12.88	12.94
Solute carrier family 2 (urate transporter), member 9	Slc2a9	12.42	10.74
Solute carrier family 25 (mitochondrial carrier, adenine nucleotide translocator), member 4	Slc25a4	12.42	12.54
Solute carrier family 16 (monocarboxylic acid transporters), member 7	Slc16a7	12.12	11.52
Solute carrier family 2 (facilitated glucose transporter), member 1 (GLUT1)	Slc2a1	12.10	12.73
Solute carrier family 12, member 3 (NCC)	Slc12a3	10.77	5.28 ^a
Solute carrier family 25 (mitochondrial carrier oxoglutarate carrier) member 11	Slc25a11	10.13	10.66
Solute carrier family 27 (fatty acid transporter), member 1	Slc27a1	10.12	10.46
Solute carrier family 25 (mitochondrial carnitine/acylcarnitine translocase) member 20	Slc25a20	10.07	10.59
Solute carrier family 25 (mitochondrial carrier; phosphate carrier) member 23	Slc25a23	9.76	9.59
Solute carrier family 25 (mitochondrial carrier, Aralar), member 12	Slc25a12	9.48	9.66
Solute carrier family 5 (sodium/glucose cotransporter), Member 2 (SGLT2)	Slc5a2	9.48	9.52
Solute carrier family 25 (mitochondrial thiamine pyrophosphate carrier) member 19	Slc25a19	9.48	9.66
Solute carrier family 40 (iron-regulated transporter), member 1	Slc40a1	9.46	9.10
Solute carrier family 2 (facilitated glucose transporter), member 4 (GLUT4)	Slc2a4	9.32	8.67
Solute carrier family 25 (mitochondrial carrier ornithine transporter) member 15	Slc25a15	9.25	9.27
Solute carrier family 25, member 36	Slc25a36	9.16	9.84

Table 13 (continued)

Gene name	Gene Symbol	DCT/CNT <i>A</i> value	CCD <i>A</i> value
Solute carrier family 25, member 30	Slc25a30	9.10	8.66
Solute carrier family 11 (proton-coupled divalent metal ion transporters) member 2	Slc11a2	8.97	9.46

^a The *A* value is below the cutoff level

(Kcnj10 and Kcna1) have been recently shown to cause electrolyte imbalance in human [3, 4]. To what extent other voltage-gated channels identified in our study can participate in the physiology/pathophysiology of distal nephron and/or collecting duct remains to be established.

In subcategory *SLC* (Table 13), the most abundant transcript is pendrin (Slc26a4), a chloride/bicarbonate exchanger located at the apical membrane of the CNT and CCD cells. Also highly abundant is Slc2a9, a recently identified urate transporter [72]. Interestingly, analysis of the *SLC*(s) expressed in the DCT/CNT and/or the CCD revealed the presence of several transcripts whose expression was previously considered as restricted to the proximal tubule or to Henle's loop. For example, a high expression of the glucose transporter Glut1 (Slc2a1) and the sodium glucose cotransporter SglT2 (Slc2a5) and a moderate expression of the sodium potassium chloride cotransporter NKCC2 (Slc12a1) and the sodium phosphate cotransporter

NaPi-IIa (Slc34a2) were detected in distal nephron. Glut1 and NKCC2 transcripts were also detected in the IMCD transcriptome [11]. Expression of NaPi-IIa, NKCC2, and SglT2 in the DCT has been validated by RT-PCR analysis (D. Firsov, unpublished observations). The correlation between transcript and protein expression of these genes remains unknown. However, this information might be important for selection of tissue-specific promoters in transgenic experiments.

Transcription factors

More than 1,000 transcription factors are expressed in DCT/CNT and/or CCD above median levels (Table 14 and Supplemental Table 8). Only a small fraction of them has been assigned to a specific renal function. For instance, Homeobox-containing transcriptional factors (*Hox*) are largely involved in morphogenesis of different parts of the

Table 14 Transcription factors

Gene name	Gene Symbol	DCT/CNT <i>A</i> value	CCD <i>A</i> value
Zinc finger protein 526	Zfp526	13.23	13.31
Ring-box 1	Rbx1	13.04	13.19
Pituitary tumor-transforming gene 1	Pttg1	12.79	12.76
Mortality factor 4 like 1	Morf4l1	12.76	13.05
Jun proto-oncogene-related gene d	Jund	12.74	12.75
Homeo box D8	Hoxd8	12.66	12.80
Early growth response 1	Egr1	12.64	13.46
TSC22 domain family, member 1	Tsc22d1	12.38	12.51
Homeo box D9	Hoxd9	12.37	12.50
Jun oncogene	Jun	12.28	12.83
FBJ osteosarcoma oncogene	Fos	12.25	12.85
Nascent polypeptide-associated complex alpha polypeptide	Naca	12.17	12.64
Endothelial differentiation-related factor 1	Edf1	12.14	12.37
SUB1 homolog (<i>S. cerevisiae</i>)	Sub1	11.81	12.28
Ring finger protein 7	Rnf7	11.67	12.20
Ecotropic viral integration site 1	Evi1	11.64	12.07
Pleomorphic adenoma gene-like 1	Plagl1	11.62	11.83
MPN domain containing	Mpnd	11.57	11.89
Peroxisome proliferative-activated receptor, gamma, coactivator 1 alpha	Ppargc1a	11.55	11.37
Kruppel-like factor 9	Klf9	11.52	11.44

Table 15 Transcripts enriched in DCT/CNT

Gene name	Gene Symbol	Enrichment Factor
Solute carrier family 12, member 3	Slc12a3	44.74
Homeo box C10	Hoxc10	25.21
Secreted frizzled-related protein 1	Sfrp1	19.67
Secreted frizzled-related protein 1	Sfrp1	15.46
Homeo box A9	Hoxa9	15.33
ATP-binding cassette, subfamily A (ABC1), member 13	Abca13	15.26
Cytochrome P450, family 2, subfamily j, polypeptide 11	Cyp2j11	14.59
Secreted frizzled-related protein 1	Sfrp1	14.56
Solute carrier family 8 (sodium/calcium exchanger), member 1	Slc8a1	13.00
Predicted gene, EG653016	EG653016	12.91
Homeo box D10	Hoxd10	12.76
Sal-like 1 (<i>Drosophila</i>)	Sall1	12.62
Solute carrier family 8 (sodium/calcium exchanger), member 1	Slc8a1	12.26
Secreted frizzled-related protein 1	Sfrp1	11.51
Parvalbumin	Pvalb	11.49
Homeo box D11	Hoxd11	10.97
Solute carrier family 8 (sodium/calcium exchanger), member 1	Slc8a1	10.96
Urate transporter	Glut9	10.58
Sulfatase 2	Sulf2	8.62
Solute carrier family 8 (sodium/calcium exchanger), member 1	Slc8a1	8.59
Homeo box A10	Hoxa10	8.53
Secreted frizzled-related protein 1	Sfrp1	8.23
Expressed sequence AI854703	AI854703	8.06
AE binding protein 1	Aebp1	7.95
Solute carrier family 8 (sodium/calcium exchanger), member 1	Slc8a1	7.72
ATP-binding cassette, subfamily A (ABC1), member 13	Abca13	7.53
Kallikrein 1	Klk1	6.75
Sodium channel, type IV, beta	Scn4b	6.66
Kallikrein 1	Klk1	6.65
Kallikrein 1-related peptidase b22	Klk1b22	6.61
Predicted gene, 100038965	100038965	6.30
RIKEN cDNA C130090K23 gene	C130090K23Rik	6.25
CD8 antigen, alpha chain	Cd8a	6.22
CD8 antigen, alpha chain	Cd8a	6.06
Solute carrier family 8 (sodium/calcium exchanger), member 1	Slc8a1	5.98
Urocanase domain containing 1	Uroc1	5.92
Parathyroid hormone 1 receptor	Pth1r	5.88
Solute carrier family 8 (sodium/calcium exchanger), member 1	Slc8a1	5.85
Kallikrein 1-related peptidase b27	Klk1b27	5.57
Klotho	Kl	5.47
Kininogen 1	Kng1	5.38
Sulfatase 2	Sulf2	5.20
V-set and transmembrane domain containing 2A	Vstm2a	4.98
RAB27A, member RAS oncogene family	Rab27a	4.97
Neurofilament, light polypeptide	Nefl	4.97
Vitamin D receptor	Vdr	4.95
Usher syndrome 1C homolog (human)	Ush1c	4.92
Calbindin 1	Calb1	4.90

Table 15 (continued)

Gene name	Gene Symbol	Enrichment Factor
c-Fos-induced growth factor /// similar to FIGF	Figf	4.89
c-Fos-induced growth factor	Figf	4.86
Homeo box A9	Hoxa9	4.86
Epidermal growth factor	Egf	4.83
Urocanase domain containing 1	Uroc1	4.82
Protein phosphatase 1, regulatory (inhibitor) subunit 1A	Ppp1r1a	4.81
Glutaminyl-peptide cyclotransferase (glutaminyl cyclase)	Qpct	4.81
Klotho	Klq	4.76
Solute carrier family 8 (sodium/calcium exchanger), member 1	Slc8a1	4.69
Vitamin D receptor	Vdr	4.68
FXSD domain-containing ion transport regulator 2	Fxyd2	4.52
Secreted phosphoprotein 1	Spp1	4.51
c-Fos-induced growth factor	Figf	4.45
Afamin	Afm	4.34
Transient receptor potential cation channel subfamily V, member 5	Trpv5	4.32
Homeo box A3	Hoxa3	4.15
Urate transporter	Glut9	4.09
Homeo box C9	Hoxc9	4.05
Regulator of G-protein signaling 5	Rgs5	4.00
Lymphocyte antigen 6 complex, locus A	Ly6a	3.99
Lipoprotein lipase	Lpl	3.97
FXSD domain-containing ion transport regulator 2	Fxyd2	3.96
Solute carrier family 8 (sodium/calcium exchanger), member 1	Slc8a1	3.82
Carbohydrate sulfotransferase 11	Chst11	3.75
Protein disulfide isomerase-like	Pdilt	3.74
Uromodulin	Umod	3.74
Fatty acid desaturase domain family, member 6	Fads6	3.73
Transient receptor potential cation channel, subfamily M, member 6	Trpm6	3.72
Lipoprotein lipase	Lpl	3.65
Regulator of G-protein signaling 5	Rgs5	3.61
RIKEN cDNA 2610018G03 gene	2610018G03Rik	3.57
Fatty acid binding protein 3, muscle and heart	Fabp3	3.54
RIKEN cDNA 5033421C21 gene	5033421C21Rik	3.53
Kallikrein 1-related peptidase b16	Klk1b16	3.42
Uromodulin	Umod	3.42
Major facilitator superfamily domain containing 4	Mfsd4	3.42
Clusterin	Clu	3.40
RAB27A, member RAS oncogene family	Rab27a	3.40
Regulator of G-protein signaling 5	Rgs5	3.38
Signal peptide, CUB domain, EGF-like 3	Scube3	3.38
Small nucleolar RNA, C/D box 116 cluster	Snord116	3.36
Synaptic vesicle glycoprotein 2 a	Sv2a	3.33
Major facilitator superfamily domain containing 4	Mfsd4	3.33
AE binding protein 1	Aebp1	3.32
Tropomyosin 2, beta	Tpm2	3.31
Serine/threonine kinase 32B	Stk32b	3.30
Kallikrein 1-related peptidase b5	Klk1b5	3.30
Kallikrein 1 /// kallikrein 1-related peptidase b5	Klk1 /// Klk1b5	3.29

Table 15 (continued)

Gene name	Gene Symbol	Enrichment Factor
FXYP domain-containing ion transport regulator 2	Fxyd2	3.29
Carbohydrate sulfotransferase 11	Chst11	3.28
Kallikrein 1-related peptidase b5	Klk1b5	3.28
Sema domain, immunoglobulin domain (Ig), transmembrane domain (TM), and short cytoplasmic domain (semaphorin) 4G	Sema4g	3.27
CD8 antigen, alpha chain	Cd8a	3.26
Major urinary protein 1	Mup1	3.26
CD8 antigen, alpha chain	Cd8a	3.24
Glutathione S-transferase omega 1	Gsto1	3.23
Family with sequence similarity 19, member A5	Fam19a5	3.21
Renin 1 structural /// renin 2 tandem duplication of Ren1	Ren1 /// Ren2	3.21
Clusterin	Clu	3.20
FXYP domain-containing ion transport regulator 2	Fxyd2	3.19
Potassium channel tetramerization domain containing 12	Kctd12	3.16
S100 calcium-binding protein G	S100g	3.14
Myosin, light polypeptide 9, regulatory	Myl9	3.13
Tropomyosin 2, beta	Tpm2	3.12
Prostaglandin E receptor 3 (subtype EP3)	Ptger3	3.11
WNK lysine-deficient protein kinase 1	Wnk1	3.08
Predicted gene, EG666481	EG666481	3.08
Muscle glycogen phosphorylase	Pygm	3.07
<i>Empty</i> spiracles homolog 1 (<i>Drosophila</i>)	Emx1	3.04
Glutathione S-transferase omega 1	Gsto1	3.04
Glutathione peroxidase 6	Gpx6	3.04
Kallikrein 1-related peptidase b8	Klk1b8	3.04
Calbindin 1	Calb1	3.01
Glutathione peroxidase 3	Gpx3	3.01

renal tubule (see below). Mineralocorticoid receptor (Nr3c2), glucocorticoid receptor (Nr3c2), vitamin D receptor (Vdr), cAMP response element-binding proteins (Creb (s) and Atf(s)), peroxisome proliferator-activated receptors, TonEBP (Nfat5), Jun, Fos, Edf1, and Jag have been shown to participate in the regulation of secretion/reabsorption processes along the distal nephron and the collecting duct. Recently, we have shown that transcriptional factors of the circadian clock (arntl (bmal1), clock, npas2, dbp, hlf, tef) are playing a major role in DCT/CNT and CCD homeostatic function [10].

Comparison of DCT/CNT and CCD transcriptomes

To identify genes differentially expressed between the DCT/CNT and the CCD, we performed a comparative analysis of the normalized DCT/CNT and CCD transcriptomes. A threefold difference in expression levels and a false discovery rate of 5% were used as cutoff criteria. Overall, 122 DCT/CNT transcripts (corresponding to 82

distinct genes) and 118 CCD transcripts (corresponding to 91 distinct genes) met this criterion.

Transcripts enriched in DCT/CNT

Analysis of differentially expressed transcripts revealed two major groups of genes enriched in DCT/CNT: (1) genes of the Homeobox (*Hox*) family of transcriptional factors that play an essential role during embryonic kidney development [73] and (2) genes involved in the secretion/reabsorption of different solutes along the nephron (Table 15). The *Hox* genes have been shown to determine the segment identity of the renal tubule, being principal genes of formation and patterning of the ureteric bud and the metanephric mesenchyme. However, their role in the adult kidney is less clear. Our data demonstrate that *Hox* genes which are specifically involved in the nephron formation during the embryogenesis (*Hoxa9*, *Hoxd10*, *Hoxd11*, *Hoxa10*, *Hoxa3*, and *Hoxc9*) remain enriched in the DCT/CNT of the adult kidney [74]. In contrast, analysis

Table 16 Transcripts enriched in CCD

Gene name	Gene Symbol	Enrichment Factor
Aldehyde dehydrogenase family 1, subfamily A1	Aldh1a1	20.38
Solute carrier family 26, member 7	Slc26a7	17.92
Lipocalin 2	Lcn2	12.43
Sciellin	Scel	12.06
Disabled homolog 1 (<i>Drosophila</i>)	Dab1	10.87
Aquaporin 4	Aqp4	9.59
Disabled homolog 1 (<i>Drosophila</i>)	Dab1	9.38
E74-like factor 5	Elf5	8.81
carbohydrate (<i>N</i> -acetylgalactosamine 4-0) sulfotransferase 9	Chst9	7.75
E74-like factor 5	Elf5	7.46
Aquaporin 4	Aqp4	6.87
Disabled homolog 1 (<i>Drosophila</i>)	Dab1	6.80
Trophoblast glycoprotein	Tpbg	6.70
RAN binding protein 3-like	Ranbp31	6.55
Annexin A1	Anxa1	6.47
Gene model 106 (NCBI)	Gm106	6.33
Gamma-aminobutyric acid (GABA-A) receptor, subunit gamma 1	Gabrg1	6.33
EGF-like-domain, multiple 6	Egfl6	6.01
Aquaporin 4	Aqp4	5.99
Defensin beta 29	Defb29	5.56
Gene model 106 (NCBI)	Gm106	5.35
DNA segment, Chr 1, ERATO Doi 705, expressed	D1Ert705e	5.22
Aldehyde dehydrogenase family 1, subfamily A7	Aldh1a7	5.20
Heparan sulfate (glucosamine) 3- <i>O</i> -sulfotransferase 3B1	Hs3st3b1	4.97
Disabled homolog 1 (<i>Drosophila</i>)	Dab1	4.95
Aquaporin-2	aqp2	4.92
Solute carrier family 26, member 7	Slc26a7	4.89
NIPA-like domain containing 1	Npal1	4.89
Hypothetical LOC553095	LOC553095	4.86
S100 calcium-binding protein A14	S100a14	4.82
Fibroblast growth factor 18	Fgf18	4.66
UDP galactosyltransferase 8A	Ugt8a	4.65
Disabled homolog 1 (<i>Drosophila</i>)	Dab1	4.60
Tissue inhibitor of metalloproteinase 2	Timp2	4.59
Trophoblast glycoprotein	Tpbg	4.54
Betacellulin, epidermal growth factor family member	Btc	4.47
T-box 3	Tbx3	4.26
RIKEN cDNA D330027G24 gene	D330027G24Rik	4.25
G-protein-coupled receptor 126	Gpr126	4.23
Transmembrane and tetratricopeptide repeat containing 2	Tmtc2	4.20
Synuclein, alpha	SncA	4.15
Insulin-like growth factor 1	Igf1	4.11
Mannosyl (alpha-1,3-)-glycoprotein beta-1,4- <i>N</i> -acetylglucosaminyl transferase	Mgat4c	4.09
Synuclein, alpha	SncA	4.08
Mucin 20	Muc20	4.06
Lymphocyte cytosolic protein 2	Lcp2	4.04
Gremlin 2 homolog, cysteine knot superfamily (<i>Xenopus laevis</i>)	Grem2	4.00

Table 16 (continued)

Gene name	Gene Symbol	Enrichment Factor
RIKEN cDNA 4930523C07 gene	4930523C07Rik	4.00
RAN binding protein 3-like	Ranbp3l	3.97
Gamma-aminobutyric acid (GABA-A) receptor, subunit gamma 1	Gabrg1	3.96
NIPA-like domain containing 1	Npal1	3.86
Tissue inhibitor of metalloproteinase 2 (Timp2), mRNA	Timp2	3.86
Prostaglandin E receptor 1 (subtype EP1)	Ptger1	3.83
FXYP domain-containing ion transport regulator 4	Fxyd4	3.81
RNA binding motif, single stranded interacting protein	Rbms3	3.80
RIKEN cDNA 9330118A15 gene	9330118A15Rik	3.78
G-protein-coupled receptor 126	Gpr126	3.78
Sterile alpha motif domain containing 12	Samd12	3.73
Synaptic nuclear envelope 1	Syne1	3.73
Pre-B-cell leukemia transcription factor 3	Pbx3	3.70
cDNA sequence BC042782	BC042782	3.69
Neural cell adhesion molecule 2	Ncam2	3.69
Procollagen lysine, 2-oxoglutarate 5-dioxygenase 2	Plod2	3.66
FXYP domain-containing ion transport regulator 3	Fxyd3	3.62
Annexin A9	Anxa9	3.62
RIKEN cDNA 1200009O22 gene	1200009O22Rik	3.61
SWI/SNF related, matrix-associated, actin dependent regulator of chromatin	Smarca1	3.60
Cyclin-dependent kinase inhibitor 2B (p15, inhibits CDK4)	Cdkn2b	3.60
Tissue inhibitor of metalloproteinase 2	Timp2	3.56
Ras association (RalGDS/AF-6) domain family (N-terminal) member 10	Rassf10	3.56
Sparc/osteonectin, cwcv and kazal-like domains proteoglycan 3	Spock3	3.55
Ankyrin repeat and SOCS box-containing 4	Asb4	3.54
Glycerophosphodiester phosphodiesterase domain containing 3	Gdpd3	3.50
RIKEN cDNA 2310076G05 gene	2310076G05Rik	3.48
Sperm-associated antigen 5	Spag5	3.48
RIKEN cDNA 8430436O14 gene	8430436O14Rik	3.47
Roundabout homolog 1 (<i>Drosophila</i>)	Robo1	3.44
Aquaporin 6	Aqp6	3.41
UDP galactosyltransferase 8A	Ugt8a	3.41
Aquaporin 6	Aqp6	3.40
Phosphodiesterase 1C	Pde1c	3.40
Protein tyrosine phosphatase-like A domain containing 2	Ptplad2	3.39
Mex3 homolog B (<i>C. elegans</i>)	Mex3b	3.38
Betacellulin, epidermal growth factor family member	Btc	3.38
Aquaporin 6, mRNA (cDNA clone IMAGE:40102370)	Aqp6	3.35
Zinc finger protein 105	Zfp105	3.35
RAS-like, family 11, member A	Rasl11a	3.34
Nuclear factor I/A	Nfia	3.31
Microtubule-associated protein tau	Mapt	3.30
Nuclear factor I/A	Nfia	3.27
Integral membrane protein 2A	Itm2a	3.25
Chimerin (chimaerin) 2	Chn2	3.21
Potassium voltage-gated channel, subfamily H (eag-related), member 5	Kcnh5	3.21
Tissue inhibitor of metalloproteinase 2	Timp2	3.20
RIKEN cDNA 4930523C07	gene 4930523C07Rik	3.20

Table 16 (continued)

Gene name	Gene Symbol	Enrichment Factor
RIKEN cDNA 8430436O14	gene 8430436O14Rik	3.20
Arginase type II	Arg2	3.20
RIKEN cDNA C130071C03 gene	C130071C03Rik	3.20
Wingless-type MMTV integration site 9B	Wnt9b	3.18
Zinc finger protein 458	Zfp458	3.18
RIKEN cDNA C130071C03 gene	C130071C03Rik	3.15
RIKEN cDNA A930006K02 gene	A930006K02Rik	3.14
Family with sequence similarity 167, member A	Fam167a	3.14
Acid phosphatase-like 2	Acpl2	3.13
Dedicator of cytokinesis 10	Dock10	3.13
Zinc finger protein 711	Zfp711	3.12
Purinergic receptor P2Y, G-protein coupled, 14	P2ry14	3.12
Acetylcholinesterase	Ache	3.11
Insulin-like growth factor 1	Igf1	3.11
sarcoglycan, epsilon	Sgce	3.09
Capping protein (actin filament), gelsolin-like	Capg	3.08
Metastasis associated in colon cancer 1	Macc1	3.07
Tandem C2 domains, nuclear	Tc2n	3.05
Sorting nexin 26	Snx26	3.05
Solute carrier family 45, member 3	Slc45a3	3.03
Serine/threonine/tyrosine kinase 1	Styk1	3.03
Aldolase C, fructose-bisphosphate	Aldoc	3.02
Solute carrier family 45, member 3	Slc45a3	3.01

of the CCD-enriched transcripts (Table 16) shows that *Hox* genes specifically involved in the development of the ureteric bud are either not expressed in the CCD of the adult kidney (*Hoxd1*) or show comparable expression levels in the DCT/CNT and CCD (*Hoxb7*, *Hoxd8*) [74].

At least 15 out of 83 DCT/CNT-enriched genes have been shown to participate in renal solute homeostasis. For instance, the thiazide-sensitive sodium chloride cotransporter (NCC or Slc12a3) and the WNK1 (with-no-lysine (K)) serine/threonine kinase are critically involved in sodium/chloride reabsorption and potassium secretion in the distal nephron segments [75]. The Glut9 (Slc2a9) transporter has been recently shown as a principal transporter involved in the renal handling of urate in both human and mice [76]. A significant number of the DCT/CNT-enriched genes are involved in the transepithelial reabsorption of calcium and magnesium. These latter include the genes coding for the sodium–calcium exchanger (Slc8a1), parvalbumin (Pvalb), the tissue kallikrein (Klk1), the Pth1r, *klotho* (Kl), the *Vdr*, the calcium-binding proteins calbindin-28 K (Calb1) and S100 (S100g), the epidermal growth factor (Egf), the FXFD domain-containing ion transport regulator 2 (Fxyd2), and the transient receptor potential cation channels *Trpv5* and *Trpm6* [77]. A secreted

species of *klotho* has been shown to mediate the paracrine regulation of phosphate reabsorption in the proximal tubule [78].

This analysis also revealed several DCT/CNT-enriched transcripts potentially involved in renal solutes handling. For example, the secreted frizzled-related protein 1 (Sfrp1) belongs to a small family of secreted proteins acting as antagonist of the Wnt signaling pathway. Importantly, one of the Sfrp, namely Sfrp4, is one of the most potent tumor-derived antagonists of phosphate reabsorption in the proximal tubule. As Sfrp1 strongly expressed in the kidney in normal physiological state, we believe that this gene might be an interesting candidate for maintaining phosphate balance by the kidney. Another interesting transcript is the cytochrome P450 2j11 (Cyp2j11) which shares a high degree of homology (80%) with the human Cyp2j2 protein. Several studies have provided evidence for an association of Cyp2j2 polymorphisms with a susceptibility to essential hypertension in man [79–81]. The Cyp2j2 has been proposed to regulate renal fluid electrolyte transport by catalyzing production of *cis*-epoxyeicosatrienoic acids (EETs) from the arachidonic acid. In vitro, the EETs have been shown to inhibit the activity of ENaC [82]. However, other renal targets of EETs as well as the in vivo role of

Cyp2j2/Cyp2j11 in the kidney remain unknown. Two other remarkable DCT/CNT-enriched genes are the small GTPase Rab27a which is involved in the intracellular vesicle docking and membrane trafficking and the Uscher syndrome 1C homolog (Ush1C), a ciliary protein which contributes to establishing the sensitivity to displacement of mechanotransduction channels in the hair cells [83, 84]. The functional relevance of these two proteins in the kidney remains unclear.

Transcripts enriched in CCD

The CCD transcriptome is also enriched in transcripts involved in different stages of tubulogenesis (Table 16). These include an agonist of the frizzled receptors (Wnt9b), the enzymes of retinoic acid synthetic pathway (Aldh1a1 and Aldh1a7), the metalloproteinase inhibitor 2 (Timp2), the insulin-like growth factor 1 (Igf1), a ligand of the epidermal growth factor receptor (betacellulin), the arginase 2 (Arg2), and the axon guidance receptor homolog 1 (Robo1). Several enriched transcripts encode proteins participating in tubular water/solute transport (aqp-4, aqp-2, Fxyd4, Fxyd3, Slc26a7, and Ptger1). Interestingly, CCD cells exhibit significant expression of Gpr126, an orphan GPCR controlling the Gs/cAMP signaling pathway in Schwann cells [85]. In the kidney, neither function nor cellular localization of Gpr126 had been determined thus far. However, this receptor is expressed at high levels in mCCD cells, a model of principal cells of the collecting duct (Heidi Fodstad, unpublished microarray hybridization data, personal communication). This finding, if confirmed in human principal cells, raises an interesting possibility of using Gpr126 for bypassing malfunctioning V2R signaling pathway in X-linked nephrogenic diabetes insipidus. Both the DCT/CNT and the CCD transcriptomes are enriched by enzymes involved in sulfation of glycoproteins (Sulf2 and Chst11 in DCT/CNT and Chst9 and Hs3st3b1 in CCD). Sulfation is a posttranslational modification known to contribute to the functional heterogeneity of glycoproteins by modifying their binding capacities to glycans, glycolipids, or to other glycoproteins. In the kidney, sulfation has been shown to affect many important biological processes including immune response, cell–cell adhesion, and hormonal signaling. Yet the specific targets of the above-mentioned enzymes along the nephron and in the collecting duct remain unknown.

Overall, this in-depth analysis of the mouse transcriptomes of the DCT/CNT and CCD opens new avenues in the comprehensive interpretation of molecular mechanisms underlying renal homeostasis. More studies are needed that will decipher the exact roles and interactions of the genes expressed in the distal part of the nephron and in the CCD.

Acknowledgments This work was supported by the Swiss National Science Foundation Research Grant 3100A0-117824 (DF) and a bridge grant for young investigator from the Faculty of Biology and Medicine of the University of Lausanne and the Prof. Placide Nicod Foundation (OB). We would like to thank Dr. Hannes Richter from the Lausanne Genomic Technologies facility for the qPCR analysis of GPCRs expression levels.

References

- Kahle KT, Wilson FH, Laloti M, Toka H, Qin H, Lifton RP (2004) WNK kinases: molecular regulators of integrated epithelial ion transport. *Curr Opin Nephrol Hypertens* 13:557–562
- Meij IC, Koenderink JB, van Bokhoven H, Assink KF, Groenestege WT, de Pont JJ, Bindels RJ, Monnens LA, van den Heuvel LP, Knoers NV (2000) Dominant isolated renal magnesium loss is caused by misrouting of the Na(+),K(+)-ATPase gamma-subunit. *Nat Genet* 26:265–266
- Scholl UI, Choi M, Liu T, Ramaekers VT, Hausler MG, Grimmer J, Tobe SW, Farhi A, Nelson-Williams C, Lifton RP (2009) Seizures, sensorineural deafness, ataxia, mental retardation, and electrolyte imbalance (SeSAME syndrome) caused by mutations in KCNJ10. *Proc Natl Acad Sci USA* 106:5842–5847
- Glaudemans B, van der Wijst J, Scola RH, Lorenzoni PJ, Heister A, van der Kemp AW, Knoers NV, Hoenderop JG, Bindels RJ (2009) A missense mutation in the Kv1.1 voltage-gated potassium channel-encoding gene KCNA1 is linked to human autosomal dominant hypomagnesemia. *J Clin Invest* 119:936–942
- Groenestege WM, Thebault S, van der Wijst J, van den Berg D, Janssen R, Tejpar S, van den Heuvel LP, van Cutsem E, Hoenderop JG, Knoers NV, Bindels RJ (2007) Impaired basolateral sorting of pro-EGF causes isolated recessive renal hypomagnesemia. *J Clin Invest* 117:2260–2267
- Robert-Nicoud M, Flahaut M, Elalouf JM, Nicod M, Salinas M, Bens M, Doucet A, Wincker P, Artiguenave F, Horisberger JD, Vandewalle A, Rossier BC, Firsov D (2001) Transcriptome of a mouse kidney cortical collecting duct cell line: effects of aldosterone and vasopressin. *Proc Natl Acad Sci USA* 98:2712–2716
- Fakitsas P, Adam G, Daidie D, van Bemmelen MX, Fouladkou F, Patrignani A, Wagner U, Warth R, Camargo SM, Staub O, Verrey F (2007) Early aldosterone-induced gene product regulates the epithelial sodium channel by deubiquitylation. *J Am Soc Nephrol* 18:1084–1092
- Nielsen J, Hoffert JD, Knepper MA, Agre P, Nielsen S, Fenton RA (2008) Proteomic analysis of lithium-induced nephrogenic diabetes insipidus: mechanisms for aquaporin 2 down-regulation and cellular proliferation. *Proc Natl Acad Sci USA* 105:3634–3639
- Hoffert JD, Pisitkun T, Wang G, Shen RF, Knepper MA (2006) Quantitative phosphoproteomics of vasopressin-sensitive renal cells: regulation of aquaporin-2 phosphorylation at two sites. *Proc Natl Acad Sci USA* 103:7159–7164
- Zuber AM, Centeno G, Pradervand S, Nikolaeva S, Maquelin L, Cardinaux L, Bonny O, Firsov D (2009) Molecular clock is involved in predictive circadian adjustment of renal function. *Proc Natl Acad Sci USA* 106:16523–16528
- Uawithya P, Pisitkun T, Ruttenberg BE, Knepper MA (2008) Transcriptional profiling of native inner medullary collecting duct cells from rat kidney. *Physiol Genomics* 32:229–253
- Irizarry RA, Hobbs B, Collin F, Beazer-Barclay YD, Antonellis KJ, Scherf U, Speed TP (2003) Exploration, normalization, and summaries of high density oligonucleotide array probe level data. *Biostatistics* 4:249–264

13. Marioni JC, Mason CE, Mane SM, Stephens M, Gilad Y (2008) RNA-seq: an assessment of technical reproducibility and comparison with gene expression arrays. *Genome Res* 18:1509–1517
14. Ueland J, Yuan A, Marlier A, Gallagher AR, Karihaloo A (2009) A novel role for the chemokine receptor Cxcr4 in kidney morphogenesis: an in vitro study. *Dev Dyn* 238:1083–1091
15. Borgatti R, Marelli S, Bernardini L, Novelli A, Cavallini A, Tonelli A, Bassi MT, Dallapiccola B (2009) Bilateral frontoparietal polymicrogyria (BFPP) syndrome secondary to a 16q12.1-q21 chromosome deletion involving GPR56 gene. *Clin Genet* 76:573–576
16. Robbins MJ, Michalovich D, Hill J, Calver AR, Medhurst AD, Gloger I, Sims M, Middlemiss DN, Pangalos MN (2000) Molecular cloning and characterization of two novel retinoic acid-inducible orphan G-protein-coupled receptors (GPC5B and GPRC5C). *Genomics* 67:8–18
17. He W, Miao FJ, Lin DC, Schwandner RT, Wang Z, Gao J, Chen JL, Tian H, Ling L (2004) Citric acid cycle intermediates as ligands for orphan G-protein-coupled receptors. *Nature* 429:188–193
18. Packer RK, Curry CA, Brown KM (1995) Urinary organic anion excretion in response to dietary acid and base loading. *J Am Soc Nephrol* 5:1624–1629
19. van der Wijst J, Hoenderop JG, Bindels RJ (2009) Epithelial Mg²⁺ channel TRPM6: insight into the molecular regulation. *Magn Res* 22:127–132
20. Roberts EM, Newson MJ, Pope GR, Landgraf R, Lolait SJ, O'Carroll AM (2009) Abnormal fluid homeostasis in apelin receptor knockout mice. *J Endocrinol* 202:453–462
21. Chabardes D, Firsov D, Aarab L, Clabecq A, Bellanger AC, Siaume-Perez S, Elalouf JM (1996) Localization of mRNAs encoding Ca²⁺-inhibitable adenylyl cyclases along the renal tubule. Functional consequences for regulation of the cAMP content. *J Biol Chem* 271:19264–19271
22. Cumbay MG, Watts VJ (2005) Galphaq potentiation of adenylyl cyclase type 9 activity through a Ca²⁺/calmodulin-dependent pathway. *Biochem Pharmacol* 69:1247–1256
23. Takeda S, Lin CT, Morgano PG, McIntyre SJ, Dousa TP (1991) High activity of low-Michaelis–Menten constant 3',5'-cyclic adenosine monophosphate-phosphodiesterase isozymes in renal inner medulla of mice with hereditary nephrogenic diabetes insipidus. *Endocrinology* 129:287–294
24. Rinehart J, Kahle KT, de Los Heros P, Vazquez N, Meade P, Wilson FH, Hebert SC, Gimenez I, Gamba G, Lifton RP (2005) WNK3 kinase is a positive regulator of NKCC2 and NCC, renal cation-Cl⁻ cotransporters required for normal blood pressure homeostasis. *Proc Natl Acad Sci USA* 102:16777–16782
25. Gattineni J, Bates C, Twombly K, Dwarakanath V, Robinson ML, Goetz R, Mohammadi M, Baum M (2009) FGF23 decreases renal NaPi-2a and NaPi-2c expression and induces hypophosphatemia in vivo predominantly via FGF receptor 1. *Am J Physiol Renal Physiol* 297:F282–F291
26. Lea JP, Sands JM, McMahon SJ, Tumlin JA (1994) Evidence that the inhibition of Na⁺/K⁺-ATPase activity by FK506 involves calcineurin. *Kidney Int* 46:647–652
27. Jo I, Ward DT, Baum MA, Scott JD, Coghlan VM, Hammond TG, Harris HW (2001) AQP2 is a substrate for endogenous PP2B activity within an inner medullary AKAP-signaling complex. *Am J Physiol Renal Physiol* 281:F958–F965
28. Zhang Y, Lin DH, Wang ZJ, Jin Y, Yang B, Wang WH (2008) K restriction inhibits protein phosphatase 2B (PP2B) and suppression of PP2B decreases ROMK channel activity in the CCD. *Am J Physiol Cell Physiol* 294:C765–C773
29. Mohebbi N, Mihailova M, Wagner CA (2009) The calcineurin inhibitor FK506 (tacrolimus) is associated with transient metabolic acidosis and altered expression of renal acid–base transport proteins. *Am J Physiol Renal Physiol* 297:F499–F509
30. Wei Y, Bloom P, Gu R, Wang W (2000) Protein-tyrosine phosphatase reduces the number of apical small conductance K⁺ channels in the rat cortical collecting duct. *J Biol Chem* 275:20502–20507
31. Henn V, Edemir B, Stefan E, Wiesner B, Lorenz D, Theilig F, Schmitt R, Vossebein L, Tamma G, Beyermann M, Krause E, Herberg FW, Valenti G, Bachmann S, Rosenthal W, Klussmann E (2004) Identification of a novel A-kinase anchoring protein 18 isoform and evidence for its role in the vasopressin-induced aquaporin-2 shuttle in renal principal cells. *J Biol Chem* 279:26654–26665
32. Okutsu R, Rai T, Kikuchi A, Ohno M, Uchida K, Sasaki S, Uchida S (2008) AKAP220 colocalizes with AQP2 in the inner medullary collecting ducts. *Kidney Int* 74:1429–1433
33. Bengrine A, Li J, Awayda MS (2007) The A-kinase anchoring protein 15 regulates feedback inhibition of the epithelial Na⁺ channel. *FASEB J* 21:1189–1201
34. Gkika D, Topala CN, Chang Q, Picard N, Thebault S, Houillier P, Hoenderop JG, Bindels RJ (2006) Tissue kallikrein stimulates Ca²⁺ reabsorption via PKC-dependent plasma membrane accumulation of TRPV5. *EMBO J* 25:4707–4716
35. van Balkom BW, Savelkoul PJ, Markovich D, Hofman E, Nielsen S, van der Sluijs P, Deen PM (2002) The role of putative phosphorylation sites in the targeting and shuttling of the aquaporin-2 water channel. *J Biol Chem* 277:41473–41479
36. Lin D, Sterling H, Lerea KM, Giebisch G, Wang WH (2002) Protein kinase C (PKC)-induced phosphorylation of ROMK1 is essential for the surface expression of ROMK1 channels. *J Biol Chem* 277:44278–44284
37. Stockand JD, Bao HF, Schenck J, Malik B, Middleton P, Schlanger LE, Eaton DC (2000) Differential effects of protein kinase C on the levels of epithelial Na⁺ channel subunit proteins. *J Biol Chem* 275:25760–25765
38. Irrazabal CE, Gallazzini M, Schnetz MP, Kunin M, Simons BL, Williams CK, Burg MB, Ferraris JD (2009) Phospholipase C-gamma1 is involved in signaling the activation by high NaCl of the osmoprotective transcription factor TonEBP/OREBP. *Proc Natl Acad Sci USA* 107:906–911
39. Donaldson JG (2009) Phospholipase D in endocytosis and endosomal recycling pathways. *Biochim Biophys Acta* 1791:845–849
40. van de Graaf SF, Chang Q, Mensenkamp AR, Hoenderop JG, Bindels RJ (2006) Direct interaction with Rab11a targets the epithelial Ca²⁺ channels TRPV5 and TRPV6 to the plasma membrane. *Mol Cell Biol* 26:303–312
41. Curtis LM, Gluck S (2005) Distribution of Rab GTPases in mouse kidney and comparison with vacuolar H⁺-ATPase. *Nephron Physiol* 100:p31–p42
42. Saxena SK, Kaur S (2006) Regulation of epithelial ion channels by Rab GTPases. *Biochem Biophys Res Commun* 351:582–587
43. El-Annan J, Brown D, Breton S, Bourgoin S, Ausiello DA, Marshansky V (2004) Differential expression and targeting of endogenous Arf1 and Arf6 small GTPases in kidney epithelial cells in situ. *Am J Physiol Cell Physiol* 286:C768–C778
44. Madziva MT, Birnbaumer M (2006) A role for ADP-ribosylation factor 6 in the processing of G-protein-coupled receptors. *J Biol Chem* 281:12178–12186
45. Tamma G, Procino G, Strafino A, Bononi E, Meyer G, Paulmichl M, Formoso V, Svelto M, Valenti G (2007) Hypotonicity induces aquaporin-2 internalization and cytosol-to-membrane translocation of ICln in renal cells. *Endocrinology* 148:1118–1130
46. Klussmann E, Tamma G, Lorenz D, Wiesner B, Maric K, Hofmann F, Aktories K, Valenti G, Rosenthal W (2001) An inhibitory role of Rho in the vasopressin-mediated translocation of aquaporin-2 into cell membranes of renal principal cells. *J Biol Chem* 276:20451–20457

47. Ko B, Joshi LM, Cooke LL, Vazquez N, Musch MW, Hebert SC, Gamba G, Hoover RS (2007) Phorbol ester stimulation of RasGRP1 regulates the sodium-chloride cotransporter by a PKC-independent pathway. *Proc Natl Acad Sci USA* 104:20120–20125
48. Laroche-Joubert N, Marsy S, Luriau S, Imbert-Teboul M, Doucet A (2003) Mechanism of activation of ERK and H-K-ATPase by isoproterenol in rat cortical collecting duct. *Am J Physiol Renal Physiol* 284:F948–F954
49. Mastroberardino L, Spindler B, Forster I, Loffing J, Assandri R, May A, Verrey F (1998) Ras pathway activates epithelial Na⁺ channel and decreases its surface expression in *Xenopus* oocytes. *Mol Biol Cell* 9:3417–3427
50. Noda Y, Sasaki S (2006) Regulation of aquaporin-2 trafficking and its binding protein complex. *Biochim Biophys Acta* 1758:1117–1125
51. Mistry AC, Mallick R, Klein JD, Weimbs T, Sands JM, Frohlich O (2009) Syntaxin specificity of aquaporins in the inner medullary collecting duct. *Am J Physiol Renal Physiol* 297:F292–F300
52. Barile M, Pisitkun T, Yu MJ, Chou CL, Verbalis MJ, Shen RF, Knepper MA (2005) Large scale protein identification in intracellular aquaporin-2 vesicles from renal inner medullary collecting duct. *Mol Cell Proteomics* 4:1095–1106
53. Wang CC, Ng CP, Shi H, Liew HC, Guo K, Zeng Q, Hong W (2010) A role for VAMP8/endobrevin in surface deployment of the water channel aquaporin 2. *Mol Cell Biol* 30:333–343
54. Zeng WZ, Babich V, Ortega B, Quigley R, White SJ, Welling PA, Huang CL (2002) Evidence for endocytosis of ROMK potassium channel via clathrin-coated vesicles. *Am J Physiol Renal Physiol* 283:F630–F639
55. Forgac M, Cantley L, Wiedenmann B, Altstiel L, Branton D (1983) Clathrin-coated vesicles contain an ATP-dependent proton pump. *Proc Natl Acad Sci USA* 80:1300–1303
56. Shimkets RA, Lifton RP, Canessa CM (1997) The activity of the epithelial sodium channel is regulated by clathrin-mediated endocytosis. *J Biol Chem* 272:25537–25541
57. Sun TX, Van Hoek A, Huang Y, Bouley R, McLaughlin M, Brown D (2002) Aquaporin-2 localization in clathrin-coated pits: inhibition of endocytosis by dominant-negative dynamin. *Am J Physiol Renal Physiol* 282:F998–F1011
58. van de Graaf SF, Rescher U, Hoenderop JG, Verkaart S, Bindels RJ, Gerke V (2008) TRPV5 is internalized via clathrin-dependent endocytosis to enter a Ca²⁺ controlled recycling pathway. *J Biol Chem* 283:4077–4086
59. Harel A, Wu F, Mattson MP, Morris CM, Yao PJ (2008) Evidence for CALM in directing VAMP2 trafficking. *Traffic* 9:417–429
60. Michael L, Sweeney DE, Davies JA (2005) A role for microfilament-based contraction in branching morphogenesis of the ureteric bud. *Kidney Int* 68:2010–2018
61. Mazzochi C, Bubien JK, Smith PR, Benos DJ (2006) The carboxyl terminus of the alpha-subunit of the amiloride-sensitive epithelial sodium channel binds to F-actin. *J Biol Chem* 281:6528–6538
62. Sabolic I, Katsura T, Verbavatz JM, Brown D (1995) The AQP2 water channel: effect of vasopressin treatment, microtubule disruption, and distribution in neonatal rats. *J Membr Biol* 143:165–175
63. Morrow JS, Cianci CD, Ardito T, Mann AS, Kashgarian M (1989) Ankyrin links fodrin to the alpha subunit of Na, K-ATPase in Madin-Darby canine kidney cells and in intact renal tubule cells. *J Cell Biol* 108:455–465
64. Wei Y, Wang WH (2002) Role of the cytoskeleton in mediating effect of vasopressin and herbimycin A on secretory K channels in CCD. *Am J Physiol Renal Physiol* 282:F680–F686
65. Schwiebert EM, Mills JW, Stanton BA (1994) Actin-based cytoskeleton regulates a chloride channel and cell volume in a renal cortical collecting duct cell line. *J Biol Chem* 269:7081–7089
66. Moyer BD, Denton J, Karlson KH, Reynolds D, Wang S, Mickle JE, Milewski M, Cutting GR, Guggino WB, Li M, Stanton BA (1999) A PDZ-interacting domain in CFTR is an apical membrane polarization signal. *J Clin Invest* 104:1353–1361
67. Kraemer DM, Strizek B, Meyer HE, Marcus K, Drenckhahn D (2003) Kidney Na⁺,K⁽⁺⁾-ATPase is associated with moesin. *Eur J Cell Biol* 82:87–92
68. Tamma G, Klussmann E, Oehlke J, Krause E, Rosenthal W, Svelto M, Valenti G (2005) Actin remodeling requires ERM function to facilitate AQP2 apical targeting. *J Cell Sci* 118:3623–3630
69. Ameen N, Apodaca G (2007) Defective CFTR apical endocytosis and enterocyte brush border in myosin VI-deficient mice. *Traffic* 8:998–1006
70. Chabardes-Garonne D, Mejean A, Aude JC, Cheval L, Di Stefano A, Gaillard MC, Imbert-Teboul M, Wittner M, Balian C, Anthouard V, Robert C, Segurens B, Wincker P, Weissenbach J, Doucet A, Elalouf JM (2003) A panoramic view of gene expression in the human kidney. *Proc Natl Acad Sci USA* 100:13710–13715
71. Schroeder BC, Cheng T, Jan YN, Jan LY (2008) Expression cloning of TMEM16A as a calcium-activated chloride channel subunit. *Cell* 134:1019–1029
72. Preitner F, Bonny O, Laverriere A, Rotman S, Firsov D, Da Costa A, Metref S, Thorens B (2009) Glut9 is a major regulator of urate homeostasis and its genetic inactivation induces hyperuricosuria and urate nephropathy. *Proc Natl Acad Sci USA* 106:15501–15506
73. Patterson LT, Potter SS (2003) Hox genes and kidney patterning. *Curr Opin Nephrol Hypertens* 12:19–23
74. Patterson LT, Potter SS (2004) Atlas of *Hox* gene expression in the developing kidney. *Dev Dyn* 229:771–779
75. Yang CL, Angell J, Mitchell R, Ellison DH (2003) WNK kinases regulate thiazide-sensitive Na-Cl cotransport. *J Clin Invest* 111:1039–1045
76. Bibert S, Hess SK, Firsov D, Thorens B, Geering K, Horisberger JD, Bonny O (2009) Mouse GLUT9: evidences for a urate uniporter. *Am J Physiol Renal Physiol* 297:F612–F619
77. van de Graaf SF, Bindels RJ, Hoenderop JG (2007) Physiology of epithelial Ca²⁺ and Mg²⁺ transport. *Rev Physiol Biochem Pharmacol* 158:77–160
78. Kuro-O M (2009) Klotho. *Pflugers Arch* 4:4
79. King LM, Gainer JV, David GL, Dai D, Goldstein JA, Brown NJ, Zeldin DC, Wu SN, Zhang Y, Gardner CO, Chen Q, Li Y, Wang GL, Gao PJ, Zhu DL, Polonikov AV, Ivanov VP, Solodilova MA, Khoroshaya IV, Kozhuhov MA, Ivakin VE, Katargina LN, Kolesnikova OE (2005) Single nucleotide polymorphisms in the CYP2J2 and CYP2C8 genes and the risk of hypertension. Evidence for association of polymorphisms in CYP2J2 and susceptibility to essential hypertension. A common polymorphism G-50 T in cytochrome P450 2 J2 gene is associated with increased risk of essential hypertension in a Russian population. *Pharmacogenet Genomics* 15:7–13
80. Wu SN, Zhang Y, Gardner CO, Chen Q, Li Y, Wang GL, Gao PJ, Zhu DL, Polonikov AV, Ivanov VP, Solodilova MA, Khoroshaya IV, Kozhuhov MA, Ivakin VE, Katargina LN, Kolesnikova OE (2007) Evidence for association of polymorphisms in CYP2J2 and susceptibility to essential hypertension. A common polymorphism G-50T in cytochrome P450 2J2 gene is associated with increased risk of essential hypertension in a Russian population. *Ann Hum Genet* 71:519–525
81. Polonikov AV, Ivanov VP, Solodilova MA, Khoroshaya IV, Kozhuhov MA, Ivakin VE, Katargina LN, Kolesnikova OE (2008) A common polymorphism G-50T in cytochrome P450 2J2 gene is associated with increased risk of essential hypertension in a Russian population. *Dis Markers* 24:119–126

82. Wang S, Meng F, Xu J, Gu Y (2009) Effects of lipids on ENaC activity in cultured mouse cortical collecting duct cells. *J Membr Biol* 227:77–85
83. Grillet N, Xiong W, Reynolds A, Kazmierczak P, Sato T, Lillo C, Dumont RA, Hintermann E, Sczaniecka A, Schwander M, Williams D, Kachar B, Gillespie PG, Muller U (2009) Harmonin mutations cause mechanotransduction defects in cochlear hair cells. *Neuron* 62:375–387
84. Ullrich S (2008) Glucose-induced insulin secretion: is the small G-protein Rab27A the mediator of the K(ATP) channel-independent effect? *J Physiol* 586:5291
85. Monk KR, Naylor SG, Glenn TD, Mercurio S, Perlin JR, Dominguez C, Moens CB, Talbot WS (2009) A G protein-coupled receptor is essential for Schwann cells to initiate myelination. *Science* 325:1402–1405